PROGRESSIVE DOWNSTREAM OVERPRINTING OF GLACIALLY INDUCED QUARTZ MICROTEXTURES DURING FLUVIAL SALTATION, SALMON RIVER, BRITISH COLUMBIA AND ALASKA

by

Matthew Pippin, B.S.

A Thesis

In

Geology

Submitted to the Graduate Faculty
of Texas Tech University in
Partial Fulfillment of
the Requirements for
the Degree of

MASTER OF SCIENCES

Approved

Dustin E. Sweet
Chair of Committee

Tom M. Lehman

David W. Leverington

Mark Sheridan
Dean of the Graduate School

May, 2016

ACKNOWLEDGEMENTS

I would like to acknowledge and thank my advisor Dr. Dustin Sweet for the opportunity to be a part of research that is on the forefront of quartz grain microtextural analysis. Research done by my predecessor, David Brannan, and future thesis projects have great promise in reshaping the application of quartz grain microtextures in proglacial systems. Without the support, insight, patience, and prior knowledge of Dr. Sweet, this study would not have been possible and for these reasons I am utterly grateful. In conducting research on the scanning electron microscope, Dr. Bo Zhao and Dr. Callum Hetherington provided expertise that allowed for the timely completion of my research. Additionally, the support and feedback I received from my committee members, Dr. Tom Lehman and Dr. David Leverington, provided to be invaluable.

Through the process of research and thesis writing, many colleagues play a crucial role in research support, software expertise, and lending valuable advice. I would like to thank to following for this reason: David Brannan, Jacob Cobb, Melanie Barnes Jenna Kohn, and Zach Wilson. A special thanks to David is needed to emphasize my gratitude in his efforts to pass on firsthand knowledge on the technique and microtextural analysis used for this study.

Lastly, I would like to thank the National Science Foundation for the NSF EAR-1324818 grant bestowed upon Dr. Sweet's microtextural analysis proposal. Without the funding for travel, equipment, and scanning electron microscope research time, the completion of this research would not have been possible. Additional thanks most go to the SIPES Foundation, Brand Jacka Scholarship, and Geoscience Society for additional funding on my thesis.

Table of Contents

ABSTRACT

Scanning electron microscopy (SEM) has been used to infer sedimentary transport mechanisms through careful analysis of quartz grain microtextures since the 1960s. In previous studies, it has been found that certain microtextures are indicative of unique transport processes. This study utilizes a tripartite microtextural suite to categorize transport-induced microtextures as follows: 1) sustained high shear stress microtextures which result from the stylus effect of grain-to-grain contact in a highly viscous medium such as ice or viscous debris flow, 2) percussion microtextures created through grain-to-grain collision during saltation of bedload sediment in a low viscous medium such as water or air, and 3) polygenetic microtextures created through multiple environmental processes. This paper investigates the progressive overprinting of glacially induced microtextures during fluvial saltation as a function of transport distance in the Salmon River, British Columbia and Alaska. Furthermore, a comparison to a previous study done on the Chitina River, Alaska is made to ascertain the value of the technique among different river systems.

In evaluating the Salmon River, 10 samples were taken every 2 to 4 km, as terrain allowed, over 26 km. Quartz grains (n = 843) were analyzed via SEM. Two grain-size populations were analyzed (250-850 µm and 850-2000 µm) to assess grain size variations of microtextures. Microtextures from each grain-size population were divided by total grains observed. The subsequent microtextural ratio for the 250-850µm grain-size population was divided by the 850-2000µm grain-size population. The resulting numbers for each of the 14 microtextures observed were plotted on a logarithmic scale from 0.1 to

10. Numbers closer to 10 indicate a bias towards the smaller grain-size population. Numbers closer to 0.10 indicate a bias towards the larger grain-size population. Complete unity is indicated by a divisional result of one. Through these spider plot analyses, this study found there to be little or no bias of microtexture abundance based on grain size.

In the Salmon River, sustained high shear stress microtextures display a strong negative correlation ($R^2 = 0.93$) and decrease in occurrence frequency progressively as a function of distance downstream. Percussion microtextures display a strong positive correlation ($R^2 = 0.81$) and increase in occurrence frequency with distance downstream. Polygenetic microtextures displayed a strong positive correlation ($R^2 = 0.86$) and increased in occurrence frequency with distance downstream. Sustained high shear stress microtextures survived 26 km of fluvial transportation without additional glacial sediment input. In the Chitina River, sustained high shear stress microtextures survived 188 km of transport, but downstream glacial input likely freshened the glacial microtexture input. Due to additional glacial input in the Chitina River downstream, only the first 17 km of the river is used as a comparison to the Salmon River.

Lastly, the ratio of fluvial to glacial (F/G) microtextures in the Salmon River steadily increases over the distance of the river. This indicates that as quartz grains saltate further downstream, fluvial microtextures increase in comparison to glacial microtextures. The ever-increasing trend of the Salmon River is similar to that of the first 17 km of the Chitina River. Similar trends within the Chitina and Salmon Rivers indicate that the F/G microtextural ratio may prove useful in predicting ancient glacial fronts in two hydrologically different river systems.

LIST OF TABLES

LIST OF FIGURES

CHAPTER 1

INTRODUCTION

Scanning electron microscopy (SEM) has been widely used as an investigative tool for determining the depositional environment of sedimentary systems based upon quartz grain microtextures (Krinsley and Takahashi, 1962; Krinsley and Donahue, 1968; Krinsley and Doornkamp, 1973; Baker, 1976; Khalaf and Al-Saleh, 1982; D'Orsay and van de Poll, 1985). Numerous microtextures have been identified and described, primarily by Krinsley and Doornkamp (1973) and later Mahaney (2002), yet only a portion of these microtextures can be attributed to environmental-specific processes of grain transport. Indeed, most grain transport media (i.e. water, wind, ice, and gravity) create similar microtextures on quartz grains which illustrates the concept of "equifinality" or that multiple processes lead to the same result (Brown, 1973). Numerous other studies have demonstrated that some microtextural features are indicative of specific grain-transport processes (Baker, 1976; Whalley and Langway, 1980; D'Orsay and van de Poll, 1985; Campbell and Thompson, 1991; Mahaney, 1995; Mahaney, 2002; Mahaney and Kalm, 2000; Strand et al., 2003; Van Hoesen and Orndorff, 2004; Curry et al., 2009; Strand and Immonen, 2010; Sweet and Soreghan, 2010; Kirshner and Anderson, 2013; Immonen, 2014; Keiser et al., 2015).

Wet-based glaciers, such as the Salmon Glacier being investigated in the present study, produce a unique suite of microtextures on grain surfaces that are the result of grain-to-grain stylus effect as grains slide past each other along shear planes within the glacier and/or at the base of the glacier (e.g. Mahaney and Kalm, 2000; Mahaney, 2002). Additionally, microtextural features indicative of grain-to-grain impacts during saltation

down river have been documented through recent research (Jackson, 1996; Mahaney and Kalm, 2000; Mahaney, 2002; Sweet and Soreghan, 2010; Costa et al., 2012; Keiser et al., 2015) and experimental work (Linde and Mycielska-Dowgiałło, 1980). These impact microtextures do not occur in a single unique subaqueous environment rather in any system that allows for saltating grain-to-grain impacts (Mahaney and Kalm, 2000; Costa et al., 2013).

Previous studies indicate that quartz grains in glacio-fluvial systems contain glacially induced microtextures (i.e. stylus type features) and that these microtextures can be overprinted through fluvial transport (Jackson, 1996; Mahaney and Kalm, 2000; Brannan, 2015). Mahaney and Kalm (2000) noted that in glacio-fluvial deposits quartz grains display numerous glacially induced microtextures far removed (>100 km) from ice contact facies. Furthermore, Jackson (1996) observed fluvial percussion microtextures atop glacially induced microtextures within 1 km of distance downstream of a glacial front. These two studies provide the known end-member data sets for the presence of glacially induced microtextures in a fluvial environment. Yet, neither of these studies systematically examined a potential progressive overprinting of glacially induced microtextures as a function of river transport. Recently, Brannan (2015) investigated the systematic overprinting of glacially induced microtextures on the Chitina River in the Wrangell-St. Elias National Park and Preserve of southeast Alaska. This study found an inverse relationship between the ratio of glacially induced microtextures to fluvial transport microtextures and distance downstream. Data from this study found a positive correlation ($R^2 = 0.69$) for saltation induced microtextures and a negative correlation ($R^2 = 0.58$) of glacially induced microtextures downstream from the glacial terminus

(Brannan, 2015).

The primary goal of the present study is to systematically investigate overprinting of glacially induced microtextures through fluvial transport in the Salmon River. The hydrologic regimes of the Chitina and Salmon Rivers are quite different which allows for comparing and contrasting various transport characteristics. In the current study, glacially induced microtextures are hypothesized to decrease in occurrence frequency with distance downstream due to fluvial modification of the glacial microtextures. To test this hypothesis, controls within the glacio-fluvial system need to be constrained to eliminate the potential of grain transport histories prior to glacial entrainment.

To limit transport processes outside of glacial and fluvial environments, an appropriate research locality and controls on preparation methods are required. Quartz grains are chosen for microtextural analysis due to relative worldwide abundance, high hardness, resistance to chemical weathering, and lack of cleavage that could mimic certain microtextures such as step features (Krinsley and Doornkamp, 1973; Mahaney, 2002). First-cycle quartz, or quartz grains that record no previous transport, are a preferred requirement to limit prior imprints on the surface of quartz grains prior to glacier and Salmon River transport. Grain saltation in an eolian environment can produce v-shaped cracks similar to that resulting from fluvial saltation (Baker, 1976). To control for eolian influence, grain sizes finer than 250 μm are not examined. Additionally, the appropriate river should have minimal tributaries, and the tributaries ideally would have no glacial input. In this way, all quartz grains observed can be inferred to have no inherited microtextures resulting from transport processes other than glacial and fluvial. The length and turbidity of the river should also be significant enough to allow for

microtextures to be overprinted. Accounting for the above criteria, the Salmon River provides a sufficient natural laboratory.

If progressive overprinting of glacial microtextures occurs due to cumulative fluvial energy, the downstream record of overprinting might have use as a predictive tool to determine the extent of paleoglacial fronts. To further test this potential, variability in different rivers must be tested to determine effects of river length, hydrological power, and river physiography. Thus, the Salmon River extends the knowledge base beyond the pioneering study conducted on the Chitina River.

Development of a proxy to reconstruct paleo-ice fronts from proglacial fluvial deposits would be useful because glacial depositional successions are incomplete in the rock record due to advance and retreat of glaciers recycling evidence of older glaciers (Johnson and Hansel, 1999). The application of this technique utilized in the present study may help constrain the spatial extent and relative timing of glacial cycles throughout geologic time. Another potential application of this technique may be to reconstruct ancient physiographic features of proglacial systems. For example, if overprinting of glacial microtextures through fluvial saltation occurs in a progressive manner with distance transported, then the ratio of glacial to fluvial microtextures with respect to distance transported may be related to river physiography. Tributaries contributing to the overall sediment supply may add length of saltation time to sediment influx. Through additional saltation, quartz grains may display higher fluvial microtextures. If the increase of fluvial microtextures change the F/G microtextural ratio in an observable way, the observed change may reflect the tributary influence. In the Chitina River, the F/G microtexture ratio increased and decreased depending on the

intersection of fluvial or glacial input, respectively (Brannan, 2015). If the technique yields similar results in the Salmon River, the application to ancient depositional systems is more robust. Additionally, the Salmon River study may allow for recognition of subglacial rivers. For example, if a glacial till is studied, but the quartz grains have a relatively high percentage of fluvial microtextures, that source glacier may have had a subglacial river system.

In this study, SEM analysis is utilized to ascertain grain transport history of quartz grains liberated from Salmon Glacier into the Salmon River. Ten samples were collected from active bars along the ~26 km stretch of the Salmon River, and glacial/fluvial microtextures were recorded in relationship to distance transported downstream. Glacial microtextures survived the entire studied stretch of the Salmon River, but displayed a progressive decrease in abundance. Fluvial microtextures displayed a progressive increase from glacier terminus to the river's mouth.

CHAPTER 2

BACKGROUND OF QUARTZ GRAIN SURFACE MICROTEXTURES

2.1 Tripartite Microtextural Suites

In certain depositional environments, quartz grain surfaces are subjected to transport processes that produce an indicative set of microtextures (Krinsley and Takahashi, 1962; Krinsley and Donahue, 1968; Krinsley and Doornkamp, 1973; Mahaney, 2002). Data that connects a single type of microtexture with a unique environmental setting does not exist (Brown, 1973; Krinsley and Doornkamp, 1973; Mahaney and Kalm, 2000). As a result, utilizing suites of microtextures is a better approach (Campbell and Thompson, 1991; Mahaney and Kalm, 2000; Sweet and Soreghan, 2010; Kirshner and Anderson, 2013; Brannan, 2015; Keiser et al., 2015). Given varied transport process (i.e. glacial, eolian, and fluvial), researchers have utilized microtextures to identify environment of deposition (Mahaney and Kalm, 2000; Mahaney, 2002; Alekseeva, 2005). Campbell and Thompson (1991) proposed that glacial transport and subaqueous saltation produce identifiable microtexture suites providing the theoretical background for the tripartite microtextural suite classification proposed by Sweet and Soreghan (2010): 1) Sustained high shear stress or grain-on-grain stylus engraving, 2) Percussion or grain-to-grain impacts, and 3) Polygenetic microtextures or equifinality group (Table 2.1). Polygenetic microtextures are created through non-unique processes of equifinality, whereas sustained high shear stress and percussion microtextures are created during specific transport processes.

2.2 Sustained High Shear Stress Microtextures

Sustained high shear stress microtextures result from the stylus effect of grain-to-

grain contact in a highly viscous medium such as ice or viscous debris flow. The "stylus effect" occurs when quartz grains act as a stylus, engraving a microtexture on another grain along shear planes. Sustained high shear stress microtextures or microstriae such as deep gouging and grooving are not unique to glacial environments, but are also found in highly viscous debris flows and structural shear zones (Mahaney, 2002). The presence of sustained high shear stress microtextures are prevalent in wet-based alpine glaciers (Mahaney and Kalm, 1996, Brannan, 2015). Continental glaciers produce sustained high shear stress microtextures, but at a lower frequency than wet-based glaciers (Mahaney et al., 1988; Mahaney et al., 1996; Kirshner and Anderson, 2013; Immonmen et al., 2014; Witus et al., 2014) perhaps indicating the importance of internal shear planes created by the stick-slip movement of wet-based glaciers. Highly viscous debris flows are not common within the field area, and structural shear zones common elsewhere in the Cordillera are areal restricted here and intersect the topography as lines thus volumetrically are of minimal importance. Moreover, quartz grains are in most part first-cycle quartz and shed directly from the Salmon Glacier, thus sustained high shear stress microtextures will be considered glacial in origin for the present study.

2.3 Percussion Microtextures

Quartz grains transported in a medium such as air or water have v-shaped cracks and edge rounding created through grain-to-grain collisions during saltation (Campbell and Thompson, 1991; Mahaney and Kalm, 1995; Mahaney and Kalm, 2000; Mahaney, 2002; Sweet and Soreghan, 2010). These microtextures are grouped as percussion microtextures in this study. Saltation processes are not unique to a specific depositional environment rather indicative of several. Depositional environments that produce

percussion microtextures include fluvial (Hellend and Diffendal, 1993; Mahaney and Kalm, 2000; Mahaney, 2002; Sweet and Soreghan, 2010), eolian (Khalaf and Al-Saleh, 1982; Mazullo, 1983; Mahaney and Andres, 1991; Mahaney and Andres, 1996), and near-shore marine (Baker, 1976; Campbell and Thompson, 1991; Mahaney and Dohm, 2011) systems. To exclusively attribute percussion microtextures to fluvial saltation, sites of investigation must be controlled for eolian or near-shore marine transport. Ideally the best system for comparing sustained high shear stress microtextures to fluvial percussion microtextures would be one in which grain surfaces are only subjected to glacial and fluvial transport. In the Salmon River area, there are no eolian dunes, and the targeted grain sizes for this study are too large to have significant eolian transport on exposed bars during low river flow stages. The Salmon River runs into the Portland Canal (Fig. 3.1), and the canal is not a high energy shallow marine system, but rather a low energy tidal flat. No high-magnitude transgressive event like a tsunami has been documented in the area. Thus, for this study percussion microtextures are considered to be exclusively fluvial induced.

2.4 Polygenetic Microtextures

Polygenetic microtextures include fractures resulting in similar surface microtextures through different transport processes, and thus have the lowest significance as an environmental indicator. Conchoidal fractures, subparallel linear fractures, and breakage blocks are some of the most common. A full list of microtextures is presented in Table 2.1. Polygenetic microtextures can be created through glacial stress (Mahaney and Kalm, 2000; Mahaney, 2002), burial stress (Mazullo and Ritter, 1991), mass flow (Mahaney, 2002), grain-to-grain contact through low and high viscosity (air and water)

media (Mahaney and Andres, 1991; Campbell and Thompson, 1991; Hellend and Diffendal, 1993; Mahaney and Andres, 1996; Mahaney and Kalm, 2000; Sweet and Soreghan, 2010), meteorite impacts (Mahaney, 2002), and expansion variability in clay soil profiles (Mahaney et al., 2001; Sweet and Soreghan, 2008).

Table 2.1 Nomenclature and Characteristics of Fracture-related SEM Microtextures

Microtexture Nomenclature	Characteristics (1)	Process of Microtexture Formation (2)	Selected References
Edge rounding	Rounded edges	Percussion	Campbell and Thompson, 1991; Mahaney and Kalm, 1995; 2000; Mahaney, 2002
V-shaped cracks	V-shaped fractures of variable size and depth on grain surfaces	Percussion	Campbell and Thompson, 1991; Mahaney and Kalm, 1995; 2000; Mahaney, 2002 Mahaney and Kalm, 1995; 2000
Abrasion features	Rubbed down or worn down grain surfaces	Polygenetic	Mahaney, 2002; Mazzullo and Ritter, 1991
Arc-shaped steps	Arcuate fractures on grain surfaces, with depths typically > micrometers	Polygenetic	Campbell and Thompson, 1991; Mahaney and Kalm, 1995,2000; Mahaney, 2002
Breakage blocks	Space represented by removal of block of variable size on grain, typically on grain edge	Polygenetic	Campbell and Thompson, 1991; Helland and Diffendal, 1993
Conchoidal fractures	Smooth curved fractures with ribbed appearance	Polygenetic	Campbell and Thompson, 1991; Mahaney and Kalm, 1995; Mahaney, 2002
Fracture faces	Large, smooth and clean fractures of at least 25% of grain surface	Polygenetic	Mahaney, 2002
Linear steps	Widely spaced (>5 μm) linear fractures on grain surface	Polygenetic	Campbell and Thompson, 1991; Mahaney and Kalm, 1995; Mahaney, 2002
Sharp angular features	Distinct sharp edges on grain surface	Polygenetic	Campbell and Thompson, 1991; Mahaney and Kalm, 1995; Mahaney, 2002
Subparallel linear fractures	Lineaer fractures on grain surface typically < 5μm spacing	Polygenetic	Hellend and Diffendal, 1993; Mahaney and Kalm, 1995; 2000; Mahaney, 2002
Mechanically upturned plates	Partially torn loose plates from the mineral surface	Polygenetic	Mahaney and Kalm, 2000; Mahaey 2002
Cresentic gouges	Crescent-shaped gouges on grain surface, typically >5 μm deep	Sustained High Shear Stress	Campbell and Thompson, 1991; Mahaney et al., 1988; Mahaney, 2002
Deep troughs	Grooves >10 μm deep	Sustained High Shear Stress	Mahaney and Kalm, 1995; 2000; Mahaney, 2002
Straight grooves	Linear grooves on mineral surface <10 μm deep	Sustained High Shear Stress	Hellend and Diffendal, 1993; Mahaney and Kalm, 1995; 2000; Mahaney, 2002
Curved grooves	Curved grooves on mineral surface <10 μm deep	Sustained High Shear Stress	Hellend and Diffendal, 1993; Mahaney and Kalm, 1995; 2000; Mahaney, 2002

(1) Descriptions predominatly synthesized from Mahaney (2002)

(2) Process of microtexture divisions modified from Sweet and Soreghan (2010)

CHAPTER 3

GEOLOGIC BACKGROUND

3.1 Salmon River District Locality

The Salmon River is located in the Tongass National Forest in southeast Alaska within the Coast Mountains. To the east of Salmon River, the Bear River Ridge separates the Salmon River from the Bear River (Buddington, 1929). On the southwest side of the Salmon River, lie the Lincoln Mountains and Ninemile Mountain separated by Thumb Creek, a small tributary of Salmon River (Fig. 3.1). In general, the bedrock geology in the Salmon River drainage basin can be broadly grouped into volcanic/sedimentary deposits, igneous intrusions, and broad regional metamorphic units (Grove, 1986). The gradient of Salmon River is steep proximal (0.10) to the glacier, and diminishes abruptly (0.012) downstream from tributary confluences (Fig. 3.2).

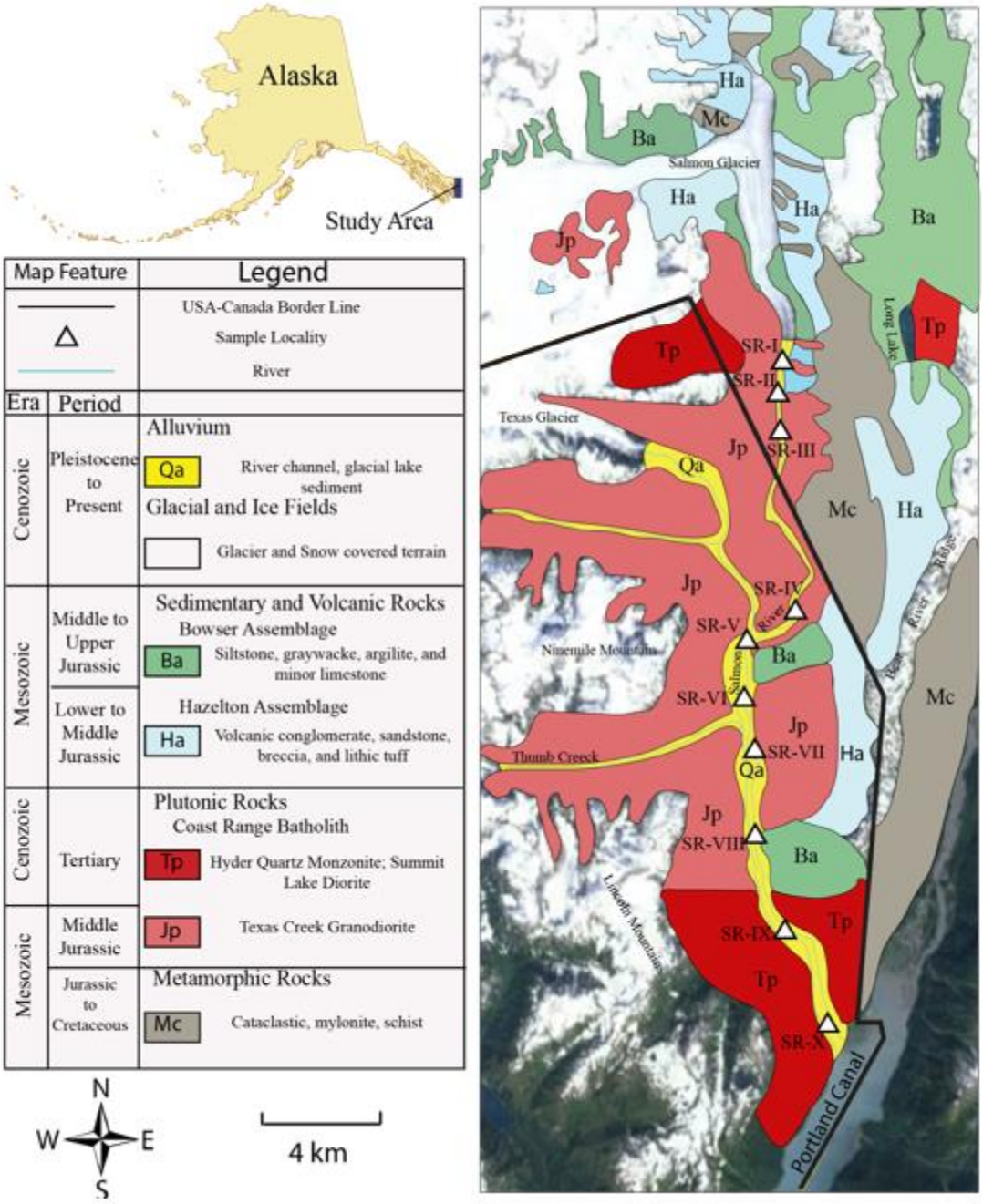

Salmon River District
Geologic Map

Figure 3.1: Salmon River district geologic map (modified from Buddington, 1929; Grove 1971). Geologic units are simplified and grouped into broad lithology of igneous, sedimentary and metamorphic assemblages and broken down by the most prominent rock type within each category.

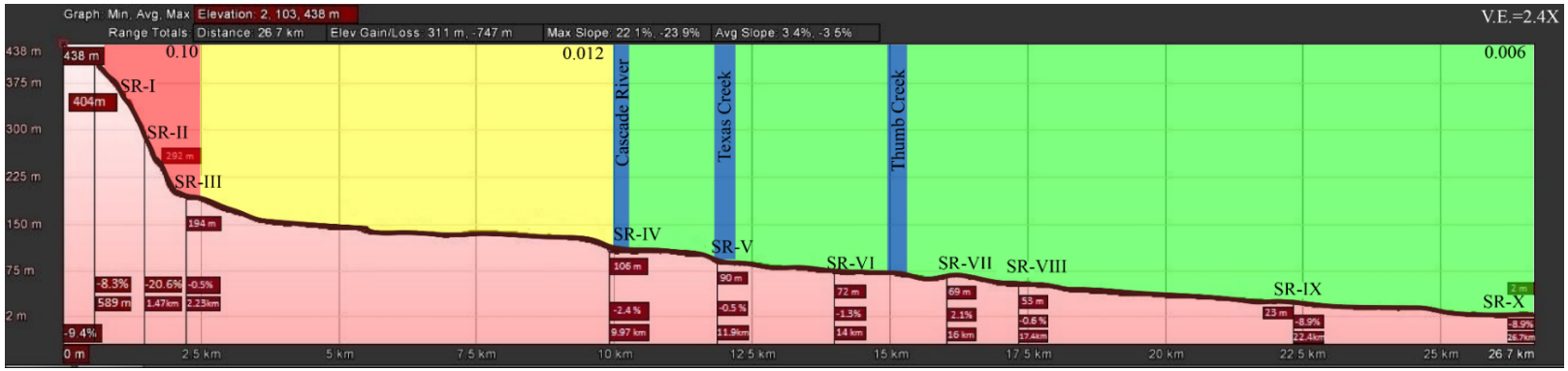

Figure 3.2: Stream elevation profile for Salmon River with sample locality. Areas shaded in red, yellow, and green indicate stream gradients of 0.10, 0.012, and 0.006, respectively. Areas shaded in blue indicate tributaries entering the Salmon River. (Modified from Google Maps, 2015)

3.2 Regional Geology

The Salmon River drainage basin exposes Jurassic calcalkaline basalt to rhyolite assemblages and volcaniclastic sedimentary rocks of the Hazelton Group (Alldrick, 1993). The Hazelton Group is divided into the Unuk River, Betty Creek, and Salmon River formations (Grove, 1986). The most detailed geologic map of the area (Grove, 1971) does not subdivide the Hazelton Group into these formations, but retains the original Hazelton and Bowser Assemblages (Fig. 3.1). The Hazelton Assemblage dominates the area north and east of Salmon Glacier and contains mostly volcanic epiclastic rocks (volcanic sandstone, breccia, conglomerate, and tuff). The majority of the Hazelton Assemblage consists of breccias with clasts of quartz, porphyritic andesite, and plagioclase whereas conglomerate and sandstone units are volumetrically minor (Grove, 1971). The Bowser Assemblage is composed primarily of siltstone and sandstone deposited in a blanket-like sheet sequentially altered by tectonism, plutonism, and erosion that create internal discontinuities and complex folding (Grove, 1971).

3.3 Geologic Events and Implications to Microtextural Analysis

3.3.1 Igneous Intrusive and Metamorphic Events

During the early Jurassic, the Texas Creek Batholith (TCB) intruded into the Salmon River area. This batholith forms the dominant provenance of first-cycle quartz in the Salmon Glacier (Fig. 3.1). The TCB ranges from a hornblende granodiorite to monzodiorite to quartz diorite and covers about 205 km^2 (Alldrick, 1993). During the Eocene, the Hyder Quartz Monzonite suite intruded the TCB and Hazelton Group near Hyder, Alaska and now bounds the east and west side of the lower Salmon River (Fig. 3.1; Grove, 1971; Alldrick, 1993). Regional metamorphism occurred in the region in the

mid-Cretaceous primarily resulting in lower greenschist facies. Later contact metamorphism was caused by intrusion of the Hyder Quartz Monzonite suite in the Eocene, but since that time the area has been less active based on the lack of metamorphism to the Hyder Quartz Monzonite (Alldrick, 1993).

3.3.2 Implications to Microtextural Analysis

The effects of metamorphic events on the Hazelton Group include the formation of cataclastic, mylonite, schist and rare gneissic rocks. All except the gneiss were formed through regional metamorphism, and the gneissic rocks are found in contact with plutons (Grove, 1986). The presence of sedimentary strata within the Salmon River watershed provides a potential for introduction of grains with ancient episodes of transport liberated from these rocks. Yet, older transport episodes recorded on grain surfaces is unlikely to affect this study because: 1) the volume of ancient sedimentary strata is limited, 2) most sedimentary strata are fine grained or volcaniclastic, and 3) regional metamorphism likely reshaped many grain surfaces. Moreover, most rocks in direct contact with Salmon Glacier are plutonic or angular volcaniclastic rocks which are potentially immature and sourced locally.

The tectonic shear zones found to the east of Salmon Glacier could have introduced grains with similar microtextures to glacial activity (c.f. Mahaney, 2002), but these areas intersect the land surface in smaller areas than igneous and sedimentary formations and have minimal contact with the glacier (Fig. 3.1). Microtextures created from the structural shear zones, associated with the regional metamorphic events, should have little influence on bedload sediment within the river.

<table>
<tr><th>Epoch</th><th>Geologic Unit</th><th>Lithology</th><th>Deposition</th><th>Tectonic Event</th><th>Geologic Event</th></tr>
<tr><td>Miocene to Holocene</td><td></td><td></td><td rowspan="2"></td><td rowspan="2">Minor faults reactivation of older faults</td><td rowspan="2">Dike complex</td></tr>
<tr><td>Oligocene</td><td>Lamprophyre Dikes</td><td>Granite, quartz monzonite, granodiorite and quartz diorite</td></tr>
<tr><td>Eocene</td><td>Hyder Batholith</td><td>Quartz monzonite and diorite</td><td>Pluton intrusion through subaerial arc volcanism</td><td>Regional doming and extension</td><td>Contact metamorphism, metasomatic and hydrothermal processes</td></tr>
<tr><td>Paleocene</td><td rowspan="3"></td><td rowspan="3"></td><td rowspan="3"></td><td>Tectonic and magmatic lull</td><td rowspan="3">No intrusive rocks
No strata preserved</td></tr>
<tr><td>Upper Cretaceous</td><td rowspan="2">Regional metamorphism
-Lower greenschist facies</td></tr>
<tr><td>Lower Cretaceous</td></tr>
<tr><td>Late Jurassic</td><td rowspan="2">Bowser Assemblage</td><td rowspan="2">Siltstone, greywacke, argillite, and minor limestone</td><td rowspan="2">Erosion of volcanics followed by marine sedimentation after subsidence</td><td>Tectonic and magmatic lull</td><td>Subsidence</td></tr>
<tr><td>Middle Jurassic</td><td rowspan="2">Texas Creek Granodiorite</td><td rowspan="2">Granodiorite</td><td rowspan="2">Pluton intrusion through subaerial arc volcanism</td><td rowspan="3">Convergent margin subduction</td><td rowspan="3">Subaqueous/Subaerial arc volcanism</td></tr>
<tr><td>Lower Jurassic</td><td rowspan="2">Hazelton Assemblage</td><td rowspan="2">Volcanic conglomerate, sandstone, breccia, and lithic tuff</td><td rowspan="2">Erosion of volcanics deposited by sedimentary processes</td></tr>
<tr><td>Upper Triassic</td><td></td><td></td><td></td></tr>
</table>

Figure 3.3: Geologic timeframe of Salmon River area, tectonic activity, and other geologic events for units contained within the study area. Lithology of units and deposition mechanism are denoted as well. Grey highlighted units contain potential 2nd cycle microtextures. (Compiled from Alldrick, 1993)

3.4 Salmon River Hydrology

The Salmon Glacier begins as a west to east trending glacier, but upon contact with mountain terrain the glacier flows mostly south forming a T-shaped profile (Fig. 3.1). Salmon Glacier dams Summit Lake on the northern boundary and heads the Salmon River on the southern boundary. Salmon Glacier is one of over 750 glaciers that dam lakes within the region and periodically cause outburst floods or "jökulhlaups" (Post and Mayo, 1971). The Salmon Glacier dams Summit Lake on the south end reducing the flow of water to the Portland Canal. The Salmon Glacier has only become self-dumping within the last fifty years which may be attributed to the retreat of ice (Mathews, 1965). In 1957, Summit Lake's surface was mapped to be 400,000 m^3/s. After the first jökulhlaup in December 1961, the lake's surface area was only 148,000 m^3/s, and Summit Lake drained 180 feet below the normal level as noted in 1957. During this flood event, mean computational discharge of the river was approximately 566 m^3/s with peak discharge around 1133 m^3/s (Mathews, 1965). Another jökulhlaup occurred in November 1965 with peak flood discharge reaching 3115 m^3/s. Prior to 1961, Salmon River experienced no documented outburst flooding as recorded from 1890 to 1960. However, from 1961 to 1971 four such events were recorded (Post and Mayo, 1971). The National Weather Service Juneau Forecast Center has recorded frequent jökulhlaups with a gauge of relative damage to the Salmon River area (Table 3.1) (Davaris, 2008). Local inhabitants of Hyder, Alaska refer to these outburst events as an annual occurrence.

Aside from catastrophic events there are at least two records of flow measurements of Salmon River taken at Ninemile Bridge before the bridge was dislodged during the 1961 flooding event. The first measurement was taken by W. H. Mathews on

June 29, 1957 and recorded a discharge of 49 m^3/sec. A second measurement was made on July 13, 1957 by the University of Toronto four miles upstream from Ninemile Bridge with a recorded flow of 42 m^3/sec. At the highest river flow on August 10, 1957, the cross-sectional area of Salmon River was 20 percent greater than on July 13, 1957 and has estimated flow of approximately 51 to 60 m^3/sec (Mathews, 1965). With an annual outburst flood of high turbulence and regular season flows of up to 60 m^3/sec, the average flow of the Salmon River should have enough energy to cause sufficient fluvial overprinting of glacially induced microtextures.

Table 3.1: Jökulhlaup Occurrence in the Salmon River					
Year	Date	Damage	Year	Date	Damage
1961	December	major road/bridge damage	1994	Aug. 29-Sep. 5	no
1963	November	no	1995	Aug. 17-22	no
1965	December	2 roads washed out	1997	Jul. 29-Aug. 3	no
1967	September	yes	1998	Jul. 21-26	no
1968	Nov. 13-19	minor	1999	Jul. 30-Aug. 5	no
1970	Aug. 2-9	3 1/2 miles of road washed out	2000	Jul. 26-30	minor
1971	Aug. 26-30	minor	2001	Aug. 9-14	no
1972	Oct.?-18	minor	2002	Jul. 26-?	no
1973	Sep. 17-22	major road damage	2003	Jul. 30-?	no
1974	Sep. 9-15	minor	2005	Jul. 31-?	minor road wash out at 9 mile
1975	Aug. 25-30	no	2006	Jul. 7-12	no
1976	Sep. 3-9	no	2007	Jul. 20-22	no
1977	Nov. 4-11	no	2008	Aug. 20-24	no

*Table taken from Southeast Alaska Jökulhlaup Report, National Weather Service Juneau Forecast Center (Davaris, 2008).

3.5 Late Quaternary History

Extent of glaciation in the panhandle region of Alaska from last glacial maximum to present time has greatly changed (Fig. 3.4). During the late Wisconsin, the Cordilleran Ice Sheet covered the extent of the panhandle region of Alaska and only the highest mountains peaks were visible (Clarke and Holdsworth, 2002). Deglaciation of this region continued through the Wisconsin until approximately 900 BP when the Little Ice Age began (Osborn and Luckman, 1988). Glacier advance from the Little Ice Age in the Coast Mountains of Alaska ceased in the eighteenth or nineteenth century, and the retreat of glaciers proceeded until modern day extent (Osborn and Luckman, 1988). The resulting landscape of the Coast Mountains is that of fjords and U-shaped valleys (Clarke and Holdsworth, 2002). These networks of valleys and fjords are potentially filled with late Quaternary sediment containing glacial sediment that can potentially be recycled into the Salmon River. In sampling the Salmon River, the three most proximal samples (SR-I to SR-III) were possibly reworked moraines left behind by the retreating Salmon Glacier. However, with the exception of late 20th century drift, in the Salmon River drainage evidence for Quaternary sediment is not documented. The highly erosive jökulhlaup events and steep slopes of the Salmon River drainage have potentially removed this sediment. No evidence for Pleistocene glacial deposits further downstream were discovered in the field area. The lack of Pleistocene deposits in the study area limits the potential of recycling older glacial deposits into the system.

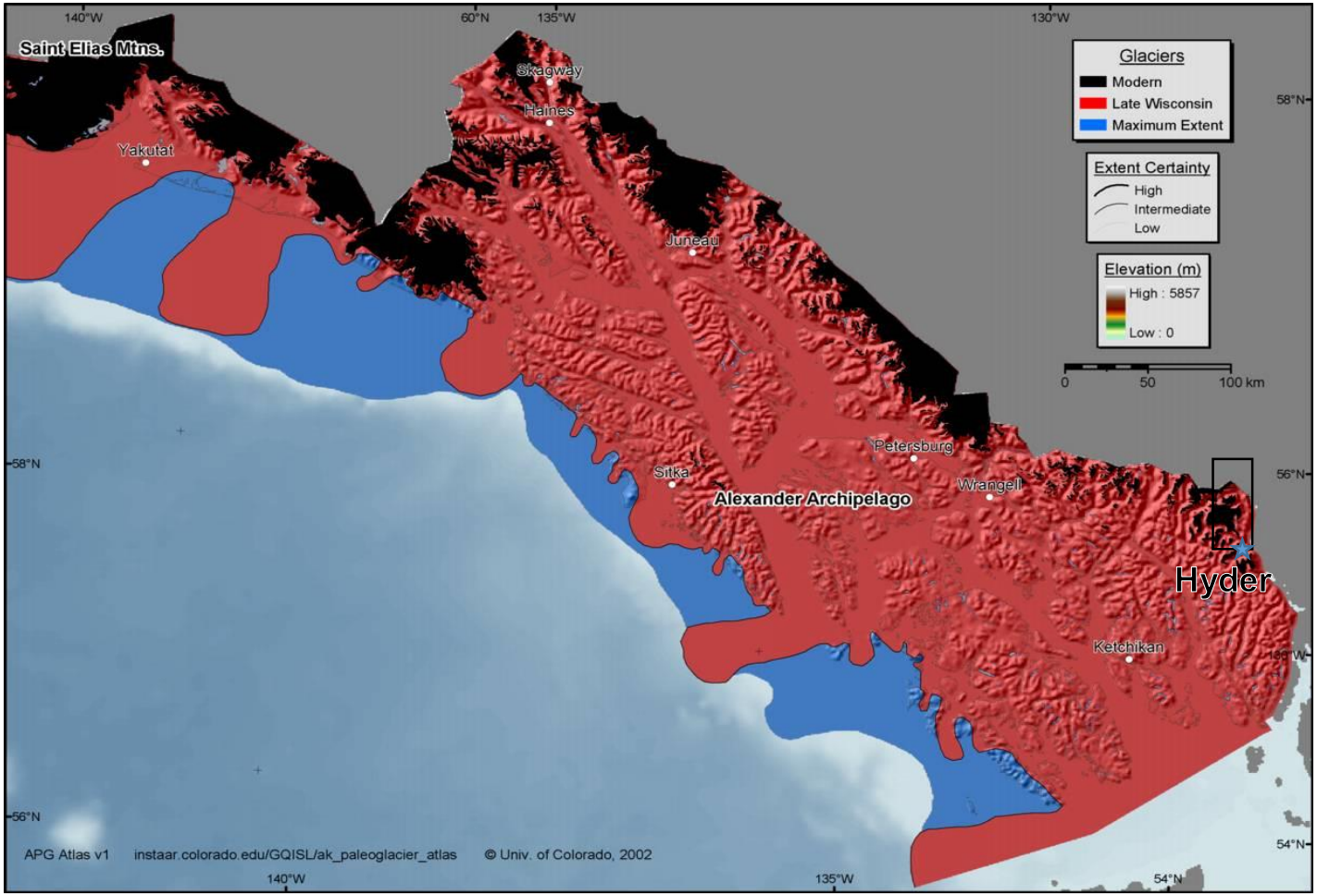

Figure 3.4: Geospatial summary of Pleistocene glaciation of southeast Alaska. The maximum extent of glaciation for the Cordilleran Ice Sheet in the last 3 million years is shown in blue. Maximum glaciation of the late Wisconsin (~20,000 years ago) is shown in red. Modern extents of glaciers are depicted in black (Manley and Kaufman, 2002). Study area is noted by a black rectangle.

CHAPTER 4

METHODS

4.1 Research Criteria

The Salmon Glacier is a wet-based glacier and is the 5th largest valley glacier in Canada (U.S. Army Corps of Engineers, 2008). The Salmon River has turbulent flow required for saltation of sand grains 250 μm to 2000 μm. The Salmon River has relatively controlled tributaries with only 3 confluences, and the Salmon River's provenance contains granodiorite and quartz monzonite. Although exposures to the east of the river and north of the Salmon Glacier contain Mesozoic coarse-grained siliciclastic and metamorphic units (Grove, 1971), as previously argued these are unlikely to produce a significant microtexture signal. The Salmon River is only 26 km in length, but according to Jackson (1996) this is enough distance to observe fluvial overprinting.

4.2 Sampling Localities of Salmon River

The Salmon River was sampled progressively every 2 to 4 km downstream except where hazardous terrain did not allow for sampling. Three samples were taken within less than 1 km apart at the terminus of the Salmon Glacier to assess proximal microtextural abundance. The next sample downstream is over 7 km because the river cuts through a steep cliff that prevents sampling safely. Samples taken before confluences are less than 2 km apart with samples downstream of confluences being approximately 4 km apart. Ten samples of bedload sediment were collected for the Salmon River. To ensure relative consistency in sediment mobility, each locality sampled was currently within the running stream along bar edges and included sediment ranging from silt-sized grains to gravel-size clasts. The sampling was completed before annual flooding occurs between June

24th, 2014 and July 3rd, 2014. Each sample taken was approximately 1 kg. Samples were labeled and located using GPS.

4.3 Sample Processing

Samples were processed in the laboratory for SEM analysis. To ensure that organic components do not hinder microtexture visibility, each sample was weighed out to approximately 30 grams in a labeled beaker and washed with 34% hydrogen peroxide until reactivity ceased. Clay particles were decanted to remove the fine-grained particles in the sediment. Upon completion of peroxide washing, each sample was gently wet sieved to avoid fracturing of the quartz grains. The samples were sieved for fine, medium, coarse, and very coarse sand populations. After sieving, the samples were heated in an oven until dry. The medium (250 μm - 850 μm) and coarse (850 μm - 2000 μm) grain-size populations were examined. The two grain-size populations are referred to as 250 μm (medium) and 850 μm (coarse) hereon.

4.4 SEM Analysis

Each sample was photographed under a binocular microscope (Fig. 4.1). Then, quartz grains were handpicked using a wet, fine-tipped brush and placed upon an SEM aluminum stub (Fig. 4.2). To maintain a non-bias selection of quartz grains, criteria for selection varied from weathered opaque to freshly fractured translucent grains and chosen at random. Furthermore, water adhesion to quartz grains is non-biased in selecting the orientation of each grain on the aluminum stubs. Each stub contained about 20-25 grains and was sputter coated with a gold-palladium mixture to reduce the charging effects from SEM analysis. Each sample was assigned an alphabetic letter in a random, non-sequential order to avoid bias in the analysis. Grains on each sample were then examined with a

Hitachi S4300 SEM (Fig. 4.3) with energy-dispersive spectrum (EDS) capabilities, tungsten filament, and 15 kV accelerating potential. All grains were verified as quartz by EDS, and the SEM microtexture atlas of Mahaney (2002) was used to identify individual microtextures. Microtextures were counted as present or not present on grain surfaces. Consequently, grains exhibiting a high abundance of a given microtexture were recorded the same as a grain that has a low abundance of the same microtexture. This ensures reproducibility of the results, eliminates subjective percent estimations, and controls potential high or low abundance outliers in the dataset. Moreover, this method is the standard technique in quartz grain microtextural analysis which allows for the data to be compared easily to other studies.

The categorization of microtextures follows the tripartite grouping of polygenetic, high sustained shear stress, and percussion as developed by Sweet and Soreghan (2010). After the presence of each microtexture was recorded, they were summed into their respective tripartite category. The total number of observations in each tripartite category for the three groups were then divided by the total number of observed microtextures. For example, if a sample contains 20 grains that have 100 polygenetic microtextures and 200 total observed microtextures, the polygenetic suite abundance of this sample would be 50%. In this way a total of observed microtextures, in terms of presence or absence per grain, are normalized into three categories and compared to each of the tripartite microtextures observed.

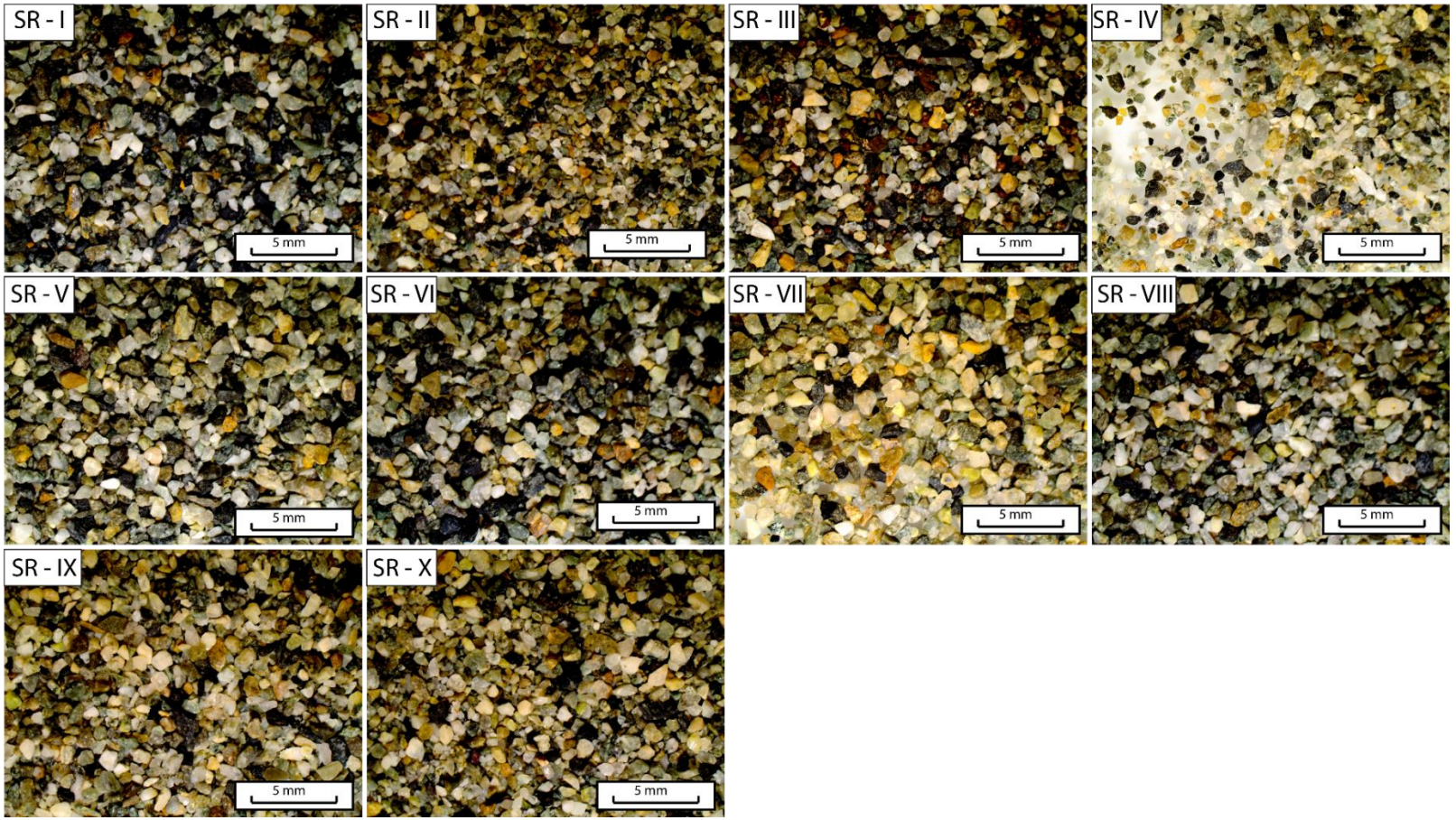

Figure 4.1: Representative Salmon River bedload sediment samples post peroxide washing for each sample locality (250 µm grain-size population).

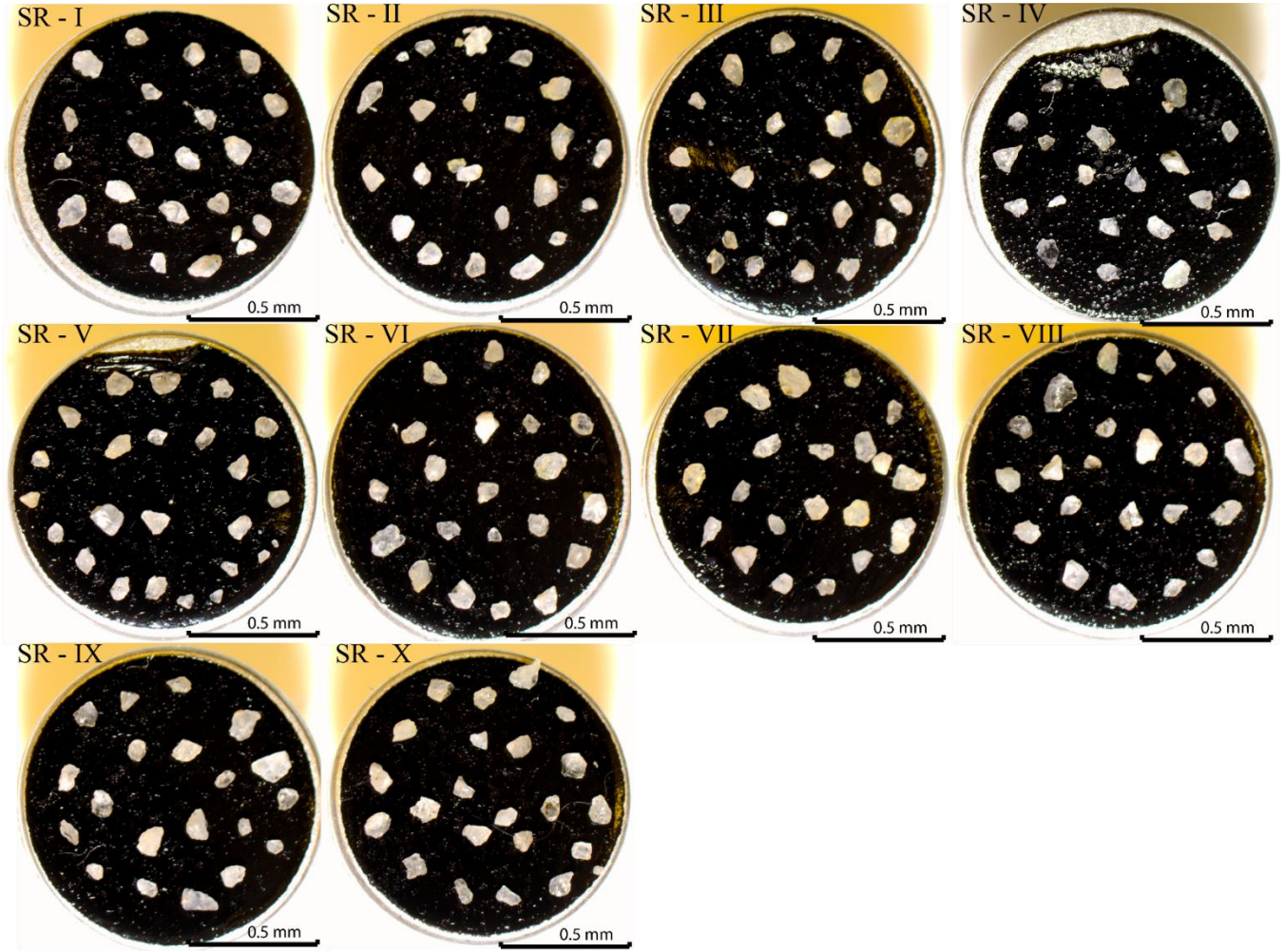

Figure 4.2: Representative aluminum stubs topped with carbon tape and quartz grains prior to gold-palladium sputter coating (250 µm grain-size population).

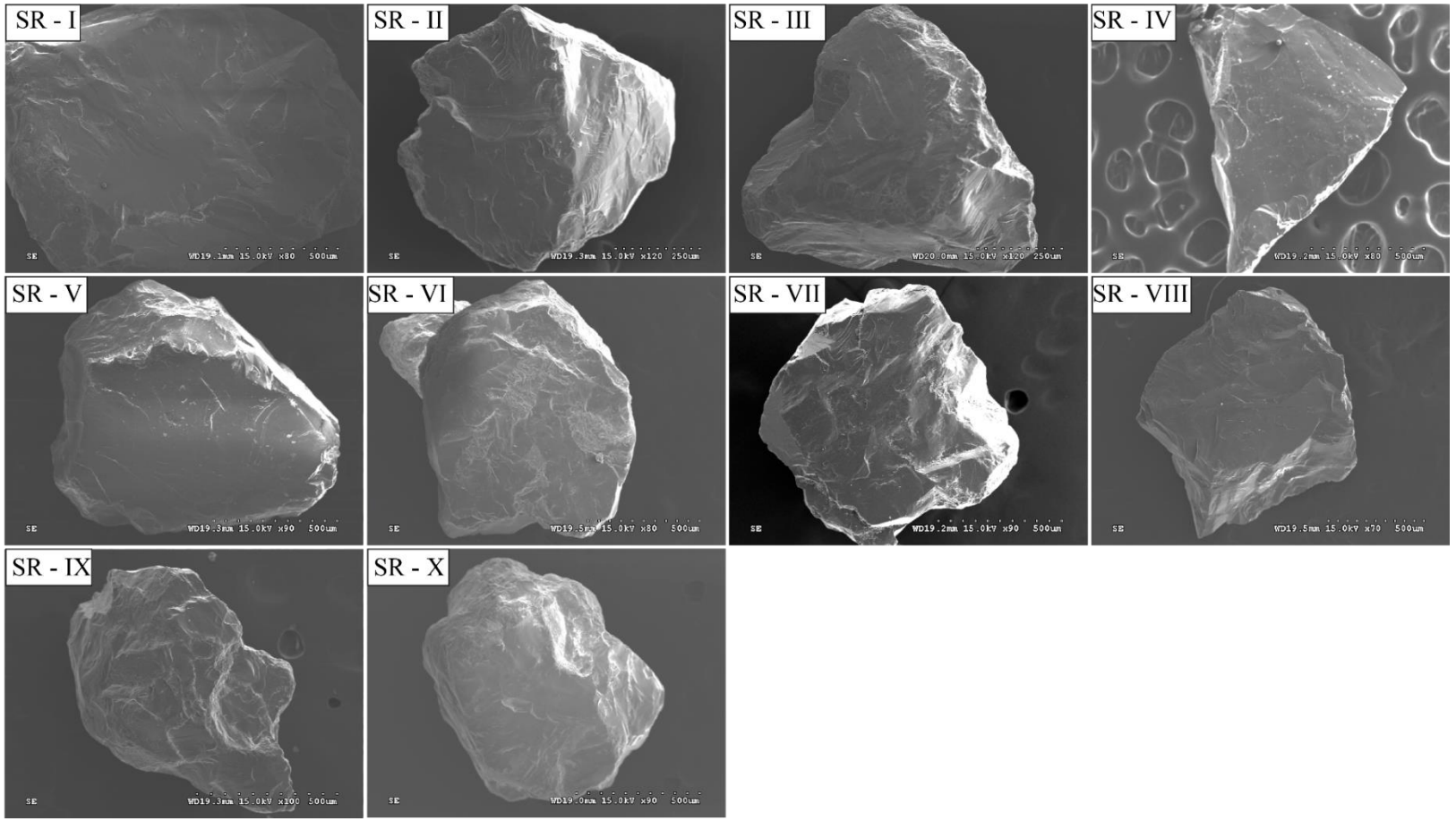

Figure 4.3: Representative micrographs of grains at sample localities along the Salmon River. Images start with proximal sample (SR-I) and progress to the furthest sample locality (SR-X). Sample distance from glacial terminus is as follows: SR-I (0.96 km), SR-II (1.83 km), SR-III (2.61 km), SR-IV (10.25 km), SR-V (12.21 km), SR-VI (13.92 km), SR-VII (15.79 km), SR-VIII (17.13 km), SR-IX (21.93 km), and SR-X (26.02 km).

4.4.1 Reproducibility of Microtextural Analysis

The technique employed on the Chitina and Salmon rivers also needs to have reproducible results. Sweet and Brannan (in press) ran a sensitivity test for three samples collected from the Chitina River, Alaska to assess the reproducibility of microtextural occurrence frequency on different grains in the same sample. In that study, samples with similar number of grains were analyzed with significant (> 6 months) time between analysis from three different localities downstream. Results suggested that within individual microtextures some variance occurred between the two runs, yet when grouped into microtextural suites, the variation of microtexture occurrence frequency was always <5% and most commonly between 1-2% (Sweet and Brannan, (in press)). Thus, microtextural occurrence frequency of quartz grains taken from the same sample is inferred reproducible through microtextural analysis in the tripartite suites.

CHAPTER 5

RESULTS

5.1 Quartz Grain Microtexture Analysis

In the Salmon River samples, quartz grains record a wide range of microtextures which adhere to Mahaney's (2002) classification and are consistent with transport-induced microtextures (Fig. 5.1). Transport of sediment within the Salmon Glacier utilizes a highly viscous medium that exhibits internal shearing and allows grains to act as a stylus producing sustained high shear stress microtextures. Once liberated into the fluvial system the transport medium (water) is lower in viscosity allowing for saltation of quartz grains which produce percussion microtextures. With only two grain transport processes present, it is inferred that all fractures observed on quartz grain surfaces are created during the interval between liberation from provenance rock to deposition on a bar in the Salmon River prior to sampling. The results of all transport microtextures analyzed are recorded in Table 5.1.

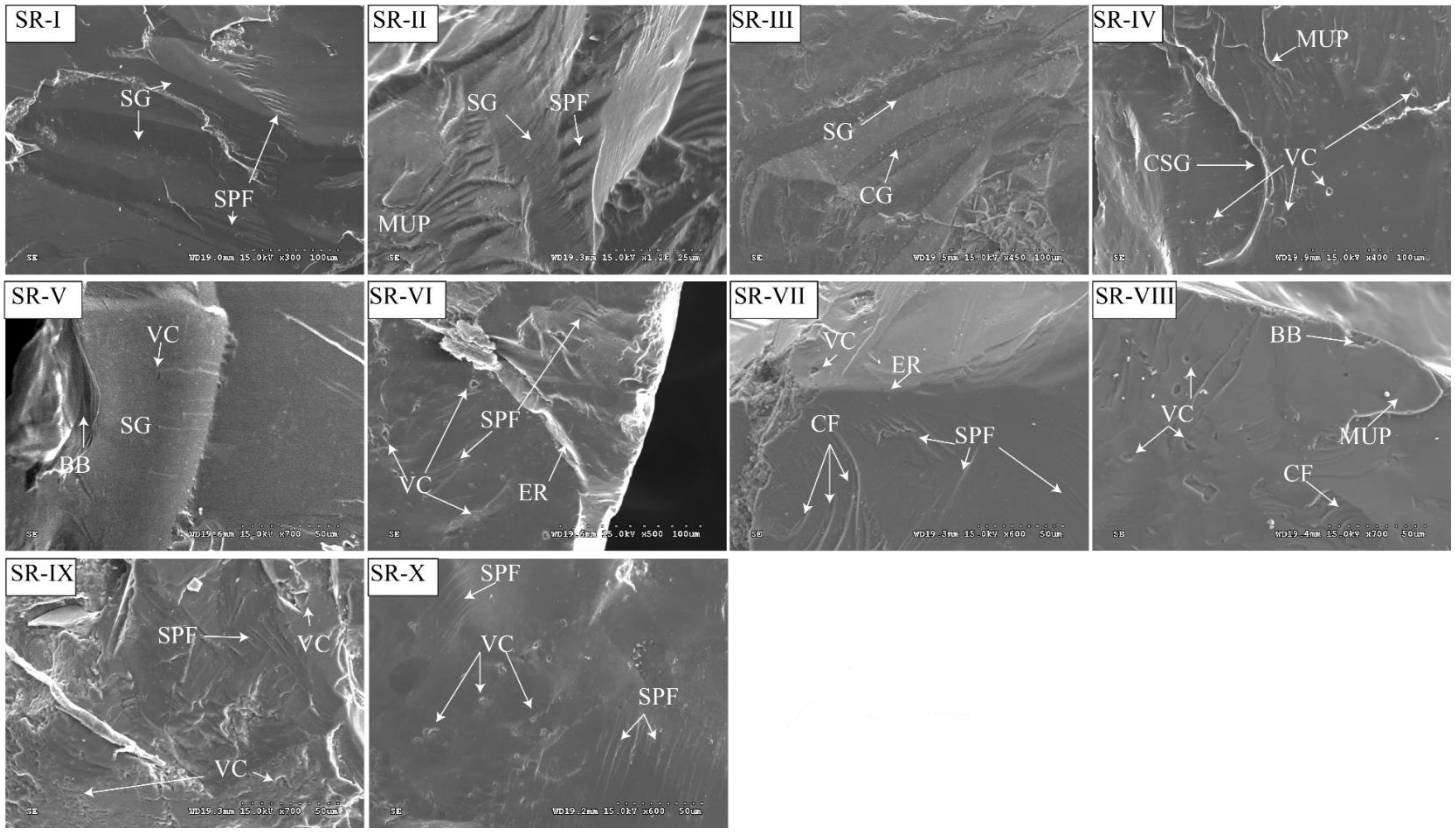

Figure 5.1: Representative micrographs for grains sampled along the Salmon River. **SR-I** (0.96 km): Straight grooves (SG) and subparallel linear fractures (SPF). **SR-II** (1.83 km): Straight groove (SG), subparallel linear fractures (SPF), and mechanically uplifted plate (MUP). **SR-III** (2.61 km): Straight groove (SG) and curved groove (CG). **SR-IV** (10.25 km): Crescentic gouge (CSG), v-shaped cracks (VC) and mechanically uplifted plate (MUP) present. **SR-V** (12.21 km): Straight groove (SG), v-shaped cracks (VC) and polygenetic fracturing of edge breakage block (BB). **SR-VI** (13.92 km) - **SR-X** (26.02 km): These samples are represented by mostly polygenetic conchoidal fractures (CF), subparallel linear fractures (SPF), breakage blocks (BB) mechanically uplifted plates (MUP) and percussion v-shaped cracks (VC) and edge rounding (ER) microtextures.

Table 5.1: Occurrence Frequency of Microtextures																
		Transport-induced microtextures														
		Polygenetic								Sustained high shear stress				Percussion	
Sample	Distance from Salmon Glacier terminus (km)	# of grains	Fracture faces	Subparallel linear fractures	Conchoidal fractures	Arc shaped steps	Linear steps	Sharp angular features	Breakage blocks	Mechanically upturned plates	Curved grooves	Straight grooves	Crescentic gouges	Deep troughs	V-shaped cracks	Edge rounding
SR-I a	0.96	38	2	28	15	7	10	2	12	26	14	16	20	0	5	22
SR-I b	0.96	35	4	31	15	6	1	4	18	28	11	13	24	2	9	18
SR-I	0.96	73	6	59	30	13	11	6	30	54	25	29	44	2	14	40
SR-II a	1.83	39	0	26	21	8	10	4	17	26	10	14	19	2	13	14
SR-II b	1.83	33	2	31	21	7	3	3	21	20	14	12	20	3	9	20
SR-II	1.83	72	2	57	42	15	13	7	38	46	24	26	39	5	22	34
SR-III a	2.61	38	1	30	12	7	1	0	22	18	11	11	15	1	8	23
SR-III b	2.61	36	0	32	19	5	3	1	19	24	5	5	20	2	14	16
SR-III	2.61	74	1	62	31	12	4	1	41	42	16	16	35	3	22	39
SR-IV a	10.25	41	10	26	32	7	10	12	19	19	9	4	21	2	24	28
SR-IV b	10.25	30	5	25	7	7	6	3	15	21	8	8	9	3	19	14
SR-IV	10.25	71	15	51	39	14	16	15	34	40	17	12	30	5	43	42
SR-V a	12.21	71	11	46	44	11	13	15	38	27	7	8	19	7	29	52
SR-V b	12.21	74	5	62	18	5	17	1	31	33	4	10	31	0	36	49
SR-V	12.21	145	16	108	62	16	30	16	69	60	11	18	50	7	65	101
SR-VI a	13.92	40	6	27	25	14	7	1	12	19	1	7	2	0	30	32
SR-VI b	13.92	39	3	33	24	2	3	5	24	20	3	4	12	0	24	28
SR-VI	13.92	79	9	60	49	16	10	6	36	39	4	11	14	0	54	60

Table 5.1: Occurrence Frequency of Microtextures																
		Transport-induced microtextures														
		Polygenetic								Sustained high shear stress				Percussion		
Sample	Distance from Salmon Glacier terminus (km)	# of grains	Fracture faces	Subparallel linear fractures	Conchoidal fractures	Arc shaped steps	Linear steps	Sharp angular features	Breakage blocks	Mechanically upturned plates	Curved grooves	Straight grooves	Crescentic gouges	Deep troughs	V-shaped cracks	Edge rounding
SR-VII a	15.79	38	9	23	15	5	4	2	16	7	5	1	10	0	10	20
SR-VII b	15.79	39	8	37	21	5	9	2	24	14	2	4	9	0	21	32
SR-VII	15.79	77	17	60	36	10	13	4	40	21	7	5	19	0	31	52
SR-VIII a	17.13	36	10	27	15	9	10	3	11	12	4	3	5	0	24	30
SR-VIII b	17.13	39	8	35	30	5	1	7	28	16	5	5	9	0	21	32
SR-VIII	17.13	75	18	62	45	14	11	10	39	28	9	8	14	0	45	62
SR-IX a	21.93	42	15	31	22	9	5	9	14	13	7	6	4	0	20	24
SR-IX b	21.93	48	7	45	36	6	5	6	31	17	3	2	3	0	31	44
SR-IX	21.93	90	22	76	58	15	10	15	45	30	10	8	7	0	51	68
SR-X a	26.02	42	8	36	31	7	10	5	17	10	1	2	3	2	28	28
SR-X b	26.02	45	5	40	37	8	9	0	29	17	1	0	4	0	30	35
SR-X	26.02	87	13	76	68	15	19	5	46	27	2	2	7	2	58	63

Gray shaded cells are combined grain-size populations

*Samples with an "a" following sample number indicate 250 µm to 850 µm sized grains

*Samples with an "b" following sample number indicate 850 µm to 2000 µm sized grains

5.1.1 Grain Size Microtextural Variance

This study analyzed between 30 and 74 grains between the two grain-size populations (i.e. 250 µm and 850 µm populations). According to Vos et al. (2014), 10 to 25 grains is the typical number of grains per sampled locality that researchers typically analyze. Microtextural variance has been suggested to vary with grain size (Krinsley and Takahashi, 1962; Margolis, 1968). To further test grain size variation two grain-size populations were prepared in this study. To assess microtextural variance as a function of grain size (i.e. 250 µm vs 850 µm), the percent of grains exhibiting specific microtextures was calculated for both grain-size populations. For example, if conchoidal fractures were observed 10 times in a sample containing 20 grains, the percentage of grains exhibiting at least one occurrence of a conchoidal fracture would be 50%. Using the percent of grains exhibiting a specific microtexture, a ratio of the 250 µm to 850 µm populations is analyzed to determine the similarity of the two populations. Ratios higher and lower than unity (i.e. ratio = 1) demonstrate more and less prevalent microtextures, respectively, in the 250 µm population. The resulting ratios are recorded (Table 5.2), then plotted on a logarithmic spider plot (Fig. 5.2), and evaluated for variation among the two grain-size populations.

Variations between the grain-size populations occur, and some ratios are unplottable due to a zero value (Fig. 5.2). Among individual microtextures, deep troughs have the most zero occurrences on grain surfaces due to a generally low abundance of observations. Fracture faces, sharp angular features, straight grooves, and curved grooves also have zero values. Of the 140 data points on the spider plot, only 8 points show variation outside a factor of five between the two size populations. Of these 8 data points,

linear steps and fracture faces have the largest variance (i.e. 8-10), and these are both microtextures within the polygenetic suite. When the variations are averaged over all sample localities (Fig. 5.2), the grain size microtextural variance is commonly within a factor of two (i.e. 0.8 – 2) displaying little variation. A slight systematic bias towards the 250 μm population may be present within linear steps (Fig. 5.2). Once the microtextures are grouped by suites indicating similar transport style (Fig. 5.3), microtexture variance is less than a factor of two in each category. Thus, because a grain size effect is minimal, or nonexistent, the data for both size populations will be grouped to better capture the natural range of microtextural variance through including more grains in a statistical population. Hereafter, the number of grains per sample ranges from 71 to 145 which is in line with the number of grains used in the Sweet and Brannan (in press) study.

Table 5.2: Ratio of Microtexture Frequency of 250 µm/ 850 µm Grain-size Populations																
			Transport-induced microtextures													
			Polygenetic								Sustained high shear stress				Percussion	
Sample	Distance from Salmon Glacier terminus (km)	# of grains	Fracture faces	Subparallel linear fractures	Conchoidal fractures	Arc shaped steps	Linear steps	Sharp angular features	Breakage blocks	Mechanically upturned plates	Curved grooves	Straight grooves	Crescentic gouges	Deep troughs	V-shaped cracks	Edge rounding
SR-I a	0.96	38	0.05	0.74	0.39	0.18	0.26	0.05	0.32	0.68	0.37	0.42	0.53	0.00	0.13	0.58
SR-I b	0.96	35	0.11	0.89	0.43	0.17	0.03	0.11	0.51	0.80	0.31	0.37	0.69	0.06	0.26	0.51
SR-I	0.96	73	0.46	0.83	0.92	1.07	9.21	0.46	0.61	0.86	1.17	1.13	0.77	-	0.51	1.13
SR-II a	1.83	39	0.00	0.67	0.54	0.21	0.26	0.10	0.44	0.67	0.26	0.36	0.49	0.05	0.33	0.36
SR-II b	1.83	33	0.06	0.94	0.64	0.21	0.09	0.09	0.64	0.61	0.42	0.36	0.61	0.09	0.27	0.61
SR-II	1.83	72	-	0.71	0.85	0.97	2.82	1.13	0.68	1.10	0.60	0.99	0.80	0.56	1.22	0.59
SR-III a	2.61	38	0.03	0.79	0.32	0.18	0.03	0.00	0.58	0.47	0.29	0.29	0.39	0.03	0.21	0.61
SR-III b	2.61	36	0.00	0.89	0.53	0.14	0.08	0.03	0.53	0.67	0.14	0.14	0.56	0.06	0.39	0.44
SR-III	2.61	74	-	0.89	0.60	1.33	0.32	-	1.10	0.71	2.08	2.08	0.71	0.47	0.54	1.36
SR-IV a	10.25	41	0.24	0.63	0.78	0.17	0.24	0.29	0.46	0.46	0.22	0.10	0.51	0.05	0.59	0.68
SR-IV b	10.25	30	0.17	0.83	0.23	0.23	0.20	0.10	0.50	0.70	0.27	0.27	0.30	0.10	0.63	0.47
SR-IV	10.25	71	1.46	0.76	3.34	0.73	1.22	2.93	0.93	0.66	0.82	0.37	1.71	0.49	0.92	1.46
SR-V a	12.21	71	0.15	0.65	0.62	0.15	0.18	0.21	0.54	0.38	0.10	0.11	0.27	0.10	0.41	0.73
SR-V b	12.21	74	0.07	0.84	0.24	0.07	0.23	0.01	0.42	0.45	0.05	0.14	0.42	0.00	0.49	0.66
SR-V	12.21	145	2.29	0.77	2.55	2.29	0.80	15.63	1.28	0.85	1.82	0.83	0.64	-	0.84	1.11
SR-VI a	13.92	40	0.15	0.68	0.63	0.35	0.18	0.03	0.30	0.48	0.03	0.18	0.05	0.00	0.75	0.80
SR-VI b	13.92	39	0.08	0.85	0.62	0.05	0.08	0.13	0.62	0.51	0.08	0.10	0.31	0.00	0.62	0.72
SR-VI	13.92	79	1.95	0.80	1.02	6.83	2.28	0.20	0.49	0.93	0.33	1.71	0.16	-	1.22	1.11

Table 5.2: Ratio of Microtexture Frequency of 250 µm/ 850 µm Grain-size Populations																
			Transport-induced microtextures													
			Polygenetic								Sustained high shear stress				Percussion	
Sample	Distance from Salmon Glacier terminus (km)	# of grains	Fracture faces	Subparallel linear fractures	Conchoidal fractures	Arc shaped steps	Linear steps	Sharp angular features	Breakage blocks	Mechanically upturned plates	Curved grooves	Straight grooves	Crescentic gouges	Deep troughs	V-shaped cracks	Edge rounding
SR-VII a	15.79	38	0.24	0.61	0.39	0.13	0.11	0.05	0.42	0.18	0.13	0.03	0.26	0.00	0.26	0.53
SR-VII b	15.79	39	0.21	0.95	0.54	0.13	0.23	0.05	0.62	0.36	0.05	0.10	0.23	0.00	0.54	0.82
SR-VII	15.79	77	1.15	0.64	0.73	1.03	0.46	1.03	0.68	0.51	2.57	0.26	1.14	-	0.49	0.64
SR-VIII a	17.13	36	0.28	0.75	0.42	0.25	0.28	0.08	0.31	0.33	0.11	0.08	0.14	0.00	0.67	0.83
SR-VIII b	17.13	39	0.21	0.90	0.77	0.13	0.03	0.18	0.72	0.41	0.13	0.13	0.23	0.00	0.54	0.82
SR-VIII	17.13	75	1.35	0.84	0.54	1.95	10.83	0.46	0.43	0.81	0.87	0.65	0.60	-	1.24	1.02
SR-IX a	21.93	42	0.36	0.74	0.52	0.21	0.12	0.21	0.33	0.31	0.17	0.14	0.10	0.00	0.48	0.57
SR-IX b	21.93	48	0.15	0.94	0.75	0.13	0.10	0.13	0.65	0.35	0.06	0.04	0.06	0.00	0.65	0.92
SR-IX	21.93	90	2.45	0.79	0.70	1.71	1.14	1.71	0.52	0.87	2.67	3.43	1.52	-	0.74	0.62
SR-X a	26.02	42	0.19	0.86	0.74	0.17	0.24	0.12	0.40	0.24	0.02	0.05	0.07	0.05	0.67	0.67
SR-X b	26.02	45	0.11	0.89	0.82	0.18	0.20	0.00	0.64	0.38	0.02	0.00	0.09	0.00	0.67	0.78
SR-X	26.02	87	1.71	0.96	0.90	0.94	1.19	-	0.63	0.63	1.07	-	0.80	-	1.00	0.86

Gray shaded cells are combined grain-size populations

*Samples with an "a" following sample number indicate 250 µm to 850 µm sized grains

*Samples with an "b" following sample number indicate 850 µm to 2000 µm sized grains

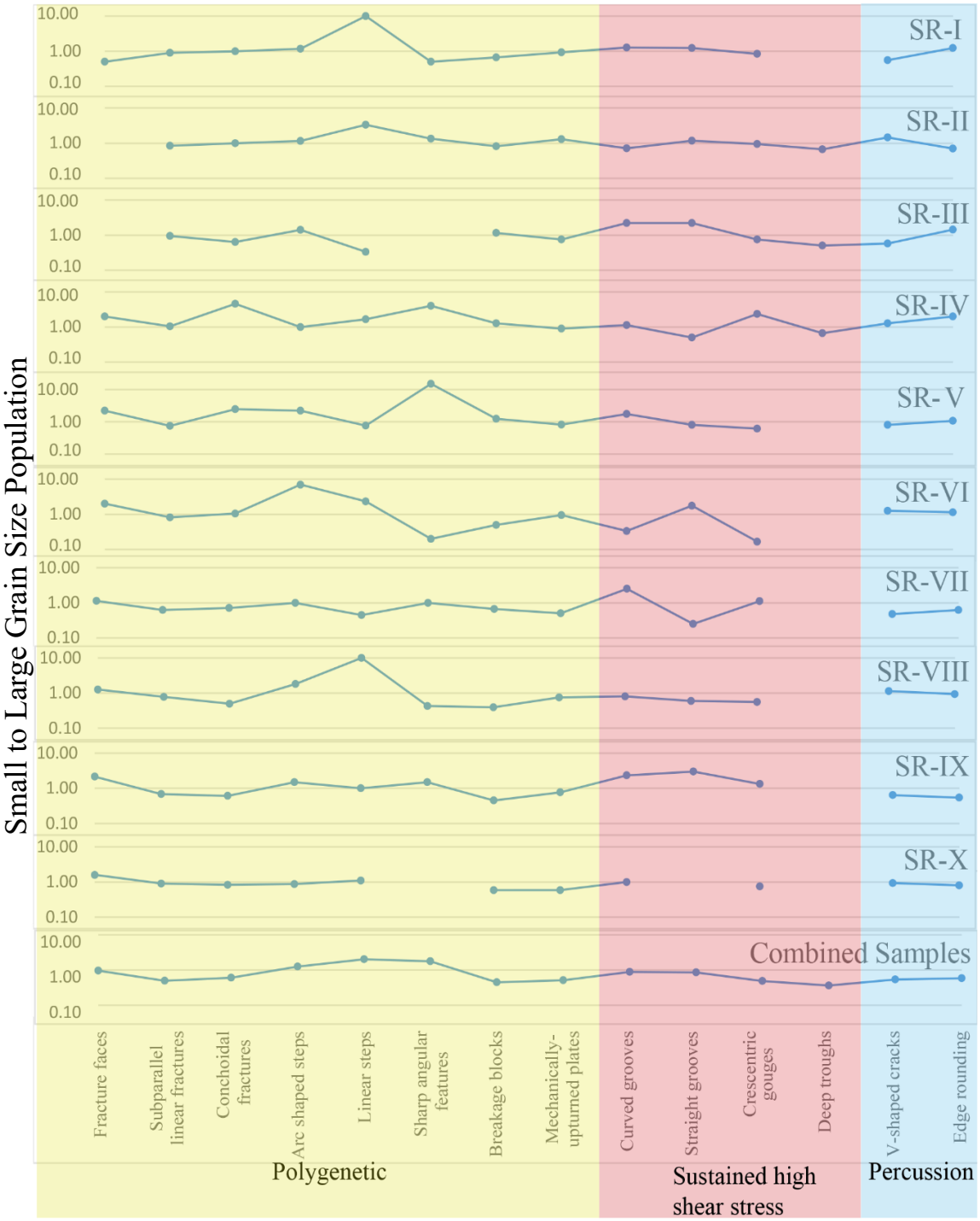

Figure 5.2: Spider plot recording microtextural variance between the 250 µm and 850 µm grain-size populations. Ratios greater than one indicate a higher abundance of microtextures recorded among the 250 µm population. Values of one indicate an even distribution of microtextures between the two size populations. Ratios less than one indicate a higher abundance of microtextures recorded among the 850 µm population.

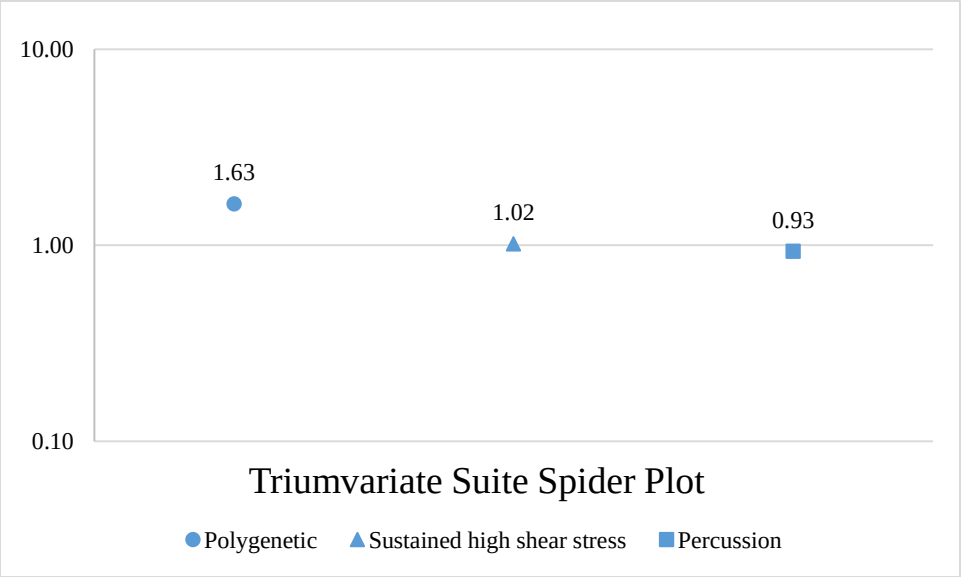

Figure 5.3: Ratio of the microtextural variance between the combined 250 µm and 850 µm grain-size populations. Ratios greater than one indicate a higher abundance of microtextures recorded among the 250 µm population. Ratios of one indicate an even distribution of microtextures between the two size populations. Ratios less than one indicate a higher abundance of microtextures recorded among the 850 µm population.

5.2 Spatial Groupings of Salmon River Samples for Microtextural Analysis

Samples collected along the Salmon River were first analyzed in spatial groupings with similar river physiography as follows: 1) Salmon Glacier terminus samples (SR-I to SR-III) and 2) samples after the Salmon River exits incised bedrock canyon and begins to form a braided channel, depending on season (SR-IV to SR-XI). The groups display differences in slope gradient and river morphology. As such, separating the samples into these two groups may elucidate variables of microtextural abundance variation.

Microtextures created by glacial and fluvial transport are classified by Sweet and Soreghan's (2010) tripartite suite. Microtextures that involve grain-to-grain contact within a highly viscous medium that impart stylized microtextures such as: crescentic gouges, grooves, and troughs are deemed to be sustained high shear stress microtextures

and in this study are considered indicative of glacial transport. Microtextures created through grain-to-grain impacts in a low viscous medium such as: edge rounding and v-shaped cracks are considered a result of saltation in the Salmon River and are termed percussion microtextures. Microtextures outside of these categories are deemed to be polygenetic and are not transport process specific. In comparing microtextures to distance downstream, this tripartite suite is referenced hereon. Within a specific tripartite category, mean and range of polygenetic, sustained high shear stress, and percussion microtextures are recorded. Grouping microtextures into these suites is becoming a common methodology in SEM microtexutral studies (e.g. Sweet and Soreghan, 2010; Kirshner and Anderson, 2013; Witus et al., 2014; Keiser et al., 2015; Sweet and Brannan (in press)).

5.2.1 Salmon River Proximal Samples (SR-I to SR-III)

The Salmon Glacier experienced advances and retreats during its history. Starting in the 1940's and 1950's, glaciers in the region have been retreating based on aerial photography (Mathews, 1965). Since the terminus of the Salmon Glacier changes position through retreat and advance, SR-I was collected as close to the terminus during June 2014 as a small ponded area prevented direct access to the current ice contact facies (Fig. 5.4). With this in mind, SR-I through SR-III will represent the most proximal samples for the current study. More specifically, samples were recovered from glacial drift (SR-I), moraine/till (SR-II), and proximal fluvial (SR-III) deposits. Over this stretch, the Salmon River displays a steep gradient of 0.10 on average, but begins to shallow downstream from sample SR-III to 0.012 (Fig. 3.2).

For the range of SR-I to SR-III, 219 angular to sub-rounded quartz grains were

examined. Samples of this group most commonly display medium relief (c.f. Mahaney, 2002) with polygenetic ($\bar{x}$ = 59%, Range = 58 to 60%), percussion ($\bar{x}$ = 16%, Range = 15 to 19%), and sustained high shear stress ($\bar{x}$ = 25%, Range = 28 to 22%) microtextural abundances. Sustained high shear stress microtextures decrease from 28% to 22% over the stretch (~1.6 km). Percussion microtextures increase in occurrence frequency downstream. The first two samples, SR-I and SR-II, have similar percussion microtexture occurrence frequency, ~15%, but SR-III has an increase to 19%.

Figure 5.4: Small ponded area directly in front of the Salmon Glacier terminus (upper-right quadrant of the photo). Location of sample SR-I.

5.2.2 Salmon River Post Tributary Samples (SR-IV to SR-X)

River morphology changes from a single incised river into a braided river with 7seasonal discharge variation from sample sites SR-IV to SR-X. A stretch of

approximately 7 km is not sampled due to inaccessibility. Of the 624 quartz grains examined in this range, grains are commonly subangular to subrounded with predominant medium surface relief under SEM. The interval distance of this group is 24.47 km, and this river reach exhibits a much shallower gradient (0.006) (Fig. 3.2).

Along this river stretch, the transport-induced microtextures have a mean and range percentage as follows: polygenetic microtextures ($\bar{x}$ = 63%, Range = 60 to 67%), percussion microtextures ($\bar{x}$ = 28%, Range = 23 to 31%), and sustained high shear stress microtextures ($\bar{x}$ = 9%, Range = 17 to 3%). Sustained high shear stress microtextures decrease downstream as a function of distance with initial occurrence frequency of 17% and ending at 3% at the river mouth. In general, percussion microtextures increase

Figure 5.5: Photograph of Texas River-Salmon River confluence. Texas River drains between the two mountains in center of view. Photograph is oriented due north and taken at 12.21 km downstream of Salmon River. Flow of Salmon River is from right to left.

downstream with a starting value of 23% and ending at 30%. At approximately 14 km downstream Texas Creek tributary sediment influx enters the Salmon River (Fig. 5.5), percussion microtextures increase to ~ 31% from 23%.

5.3 Overall Trends for the Tripartite Microtextures

Along the entire stretch of the Salmon River, 843 angular to sub-rounded quartz grains were analyzed. The tripartite microtextures, across the entire river distance, display mean and range percentage as follows: sustained high shear stress ($\bar{x}$ = 14%, Range = 28 to 3 %) percussion microtextures ($\bar{x}$ = 24%, Range = 15 to 31%), and polygenetic microtextures ($\bar{x}$ = 62%, Range = 58 to 67%). Sustained high shear stress microtextures are negatively correlated ($R^2 = 0.93$) to distance downstream from Salmon Glacier. For sustained high shear stress microtextures all occurrence frequency points are within 1σ (8%) away from the linear regressive trend line and commonly are less than 4 % away from the linear regressive trend line (Fig. 5.6). Percussion microtextures are positively correlated ($R^2 = 0.81$) to distance downstream from Salmon Glacier. Polygenetic microtextures also display a strong positive correlation ($R^2 = 0.86$) to distance downstream from Salmon Glacier. Sustained high shear stress microtextures display the greatest change in abundance range downstream (28 to 3%) and persist throughout the entire length of the river. Percussion microtextures occurrence frequency increases from 15 to 31% as a function of distance downstream, and there are zero data points outlying 1σ (~6%) (Fig. 5.6). Polygenetic microtextures have the most occurrence frequency and increase downstream from 58 to 67% with no data outlying 1σ (~3%).

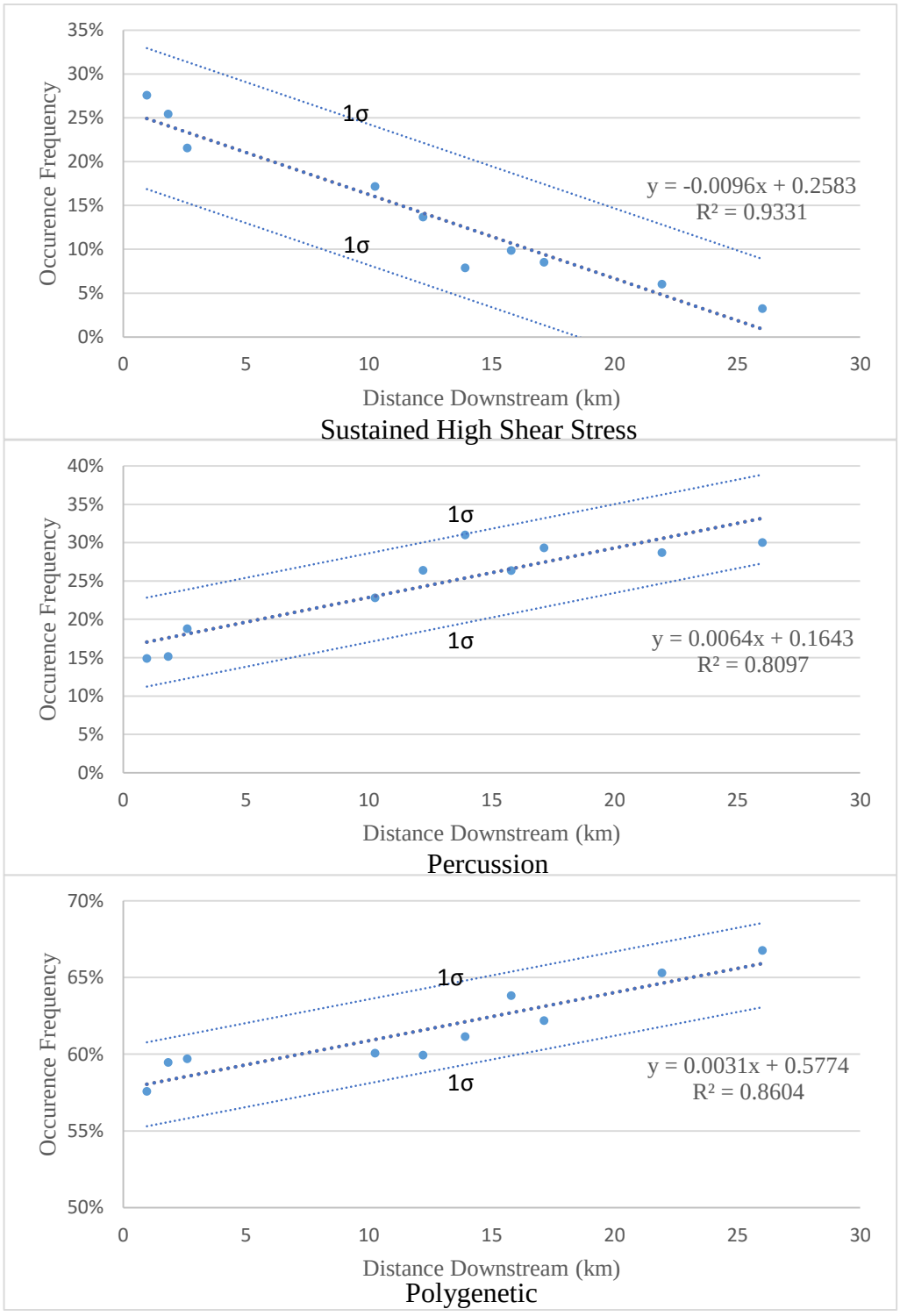

Figure 5.6: Linear regression of polygenetic, percussion, and sustained high shear stress microtextures for Salmon River. Salmon River tripartite microtextures occurrence frequency are shown for the entire length of Salmon River. The straight line equation for each data trend line and linear regression value (R^2) are noted in each plot.

CHAPTER 6

DISCUSSION

6.1 Tributary Influence on Microtextural Abundance

The Chitina River, located further to the north in the Wrangell-St. Elias National Park and Preserve, was recently sampled for a similar SEM study on quartz grain microtextures. In the Chitina River, tributaries influenced relative abundances of percussion and sustained high shear stress microtextures along the length of the river (Brannan, 2015). In that study, around 17 km downstream from the Chitina Glacier, the Chitina River intersects the terminal moraines of the Barnard and Hawkins glaciers resulting in a distinct increase in sustained high shear stress microtextural abundance (Fig. 6.1). An opposite effect was found when a tributary with significant fluvial transport distance entered the Chitina River. Sweet and Brannan (in press) found that the ratio of fluvial microtextures to glacially induced microtextures (F/G ratio) was a useful tool to demonstrate glacier and fluvial influence from tributaries. The F/G ratio of the Chitina River appeared to be sensitive enough to denote the influence of fluvial and glacial tributaries (Fig. 6.1). Accordingly, the Salmon River may also exhibit microtextural variations at confluences.

6.1.1 Sustained High Shear Stress Microtextures at Tributary Confluences

Sustained high shear stress microtextures display a strong decrease in microtextural abundance as a function of distance from the Salmon Glacier terminus. Proximal to the glacial terminus, sustained high shear stress microtextures record a relatively high

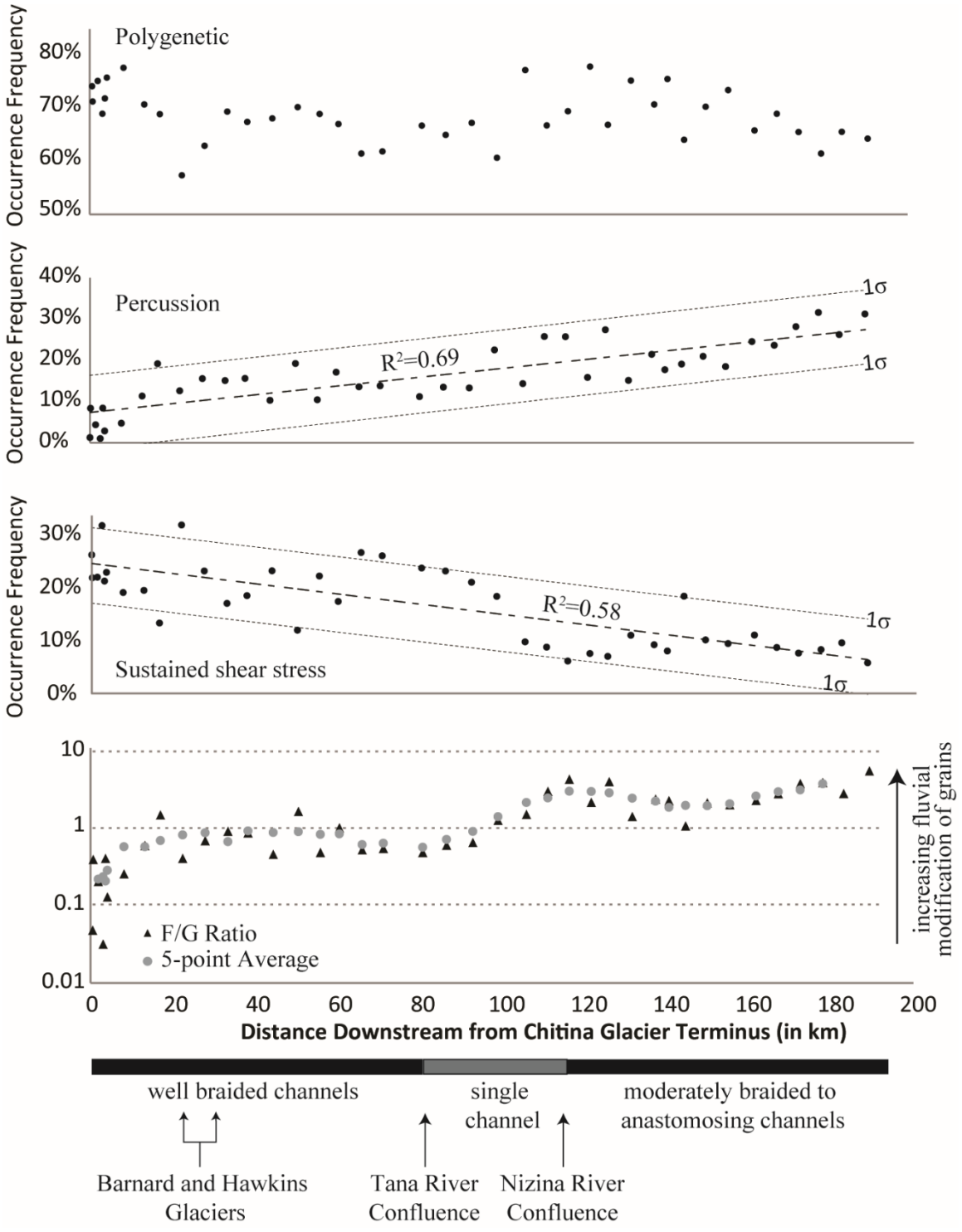

Fig. 6.1: Occurrence Frequency of the tripartite suite, percussion to fluvial (F/G) ratio, and 5-point average of the F/G ratio for the Chitina River. Localities of glaciers and river confluences are noted at the corresponding distance they are encountered downstream. (After Sweet and Brannan, (in press))

occurrence frequency (28%), but at the river mouth display a much lower frequency (3%). The progressive decrease of sustained high shear stress microtextures is uniform throughout the entire section always remaining within one standard deviation ($1\sigma = 8\%$).

The Texas Creek confluence (Fig. 5.5) does not appear to affect the abundance of sustained high shear stress microtextures. If the Texas Glacier was closer to the confluence, it is expected that sustained high shear stress microtextures would increase in abundance and closely resemble proximal samples of the Salmon River. Yet, upstream of the confluence, bedload sediment sourced from the Texas Glacier is transported approximately 9 km. Salmon Glacier bedload sediment is transported 12 km to the Texas Creek Confluence. Sample (SR-V) recovered after the Texas Creek confluence does not display greater sustained high shear stress microtextures suggesting that the similar distance of fluvial transport upstream in the Salmon River, and the Texas Creek resulted in similar abundances of percussion to sustained high stress microtextures.

The Cascade River at ~10 km and Thumb Creek at ~15 km downstream do not appear to influence the abundance of sustained high shear stress microtextures which probably reflects their relatively small size when compared to the overall Salmon River watershed. The Cascade River is not headed by a valley glacier, so it is expected that sediment deposited into the Salmon River would display an increase in percussion microtextures and potentially a decrease in those indicating sustained high shear stress. The Thumb Creek is headed by a small valley glacier, but does not result in a noticeable change in microtextural abundance at the confluence.

6.1.2 Percussion Microtextures at Tributary Confluences

Percussion microtextures represent approximately 15% of all microtextures of the proximal sample localities (SR-I to SR-III) and represent ~30% of recorded transport microtextures of braided river samples (SR-IV to SR-XI) (Fig. 5.6). No points lie outside of one standard deviation ($1\sigma = 6\%$).

Texas Creek has two forks that converge into one before entering the Salmon River system. The east fork is headed by a glacier similar to the Salmon River, but the west fork does not have a glacier and has potential to increase percussion microtextures through an additional length of river with saltating grains. Similarly, the Cascade River tributary is not headed by a glacier and could allow for an increase percussion microtextures. The combined influx of sediment between these two systems may account for the slight increase of percussion microtextures at the Texas Creek confluence (Fig. 5.6). At approximately 15 km, the Thumb Creek tributary enters the Salmon River, and at approximately 17 km percussion microtextures increase slightly, but stay within one standard deviation. These tributaries may provide sediment with higher abundance of percussion microtextures but, the magnitude of microtextural change at each confluence is also clearly within an expected range of statistical variation. Thus, the effect of tributaries is ambiguous as there are hints of increases, but within the scope of statistical variation. The tributaries for the Salmon River watershed are relatively small when compared to the tributaries that entered the Chitina River which could account for the different signal observed in the two study areas.

6.1.3 Polygenetic Microtextures at Tributary Confluences

Polygenetic microtextures display a positive correlation as a function of distance transported downstream. In general, polygenetic microtextures fall within 58 to 67%. Polygenetic microtextures tend to have a higher abundance nearer the end of the Salmon River. This increase downstream could be a function of the normalization into the three groupings. Since the abundance of percussion microtextures levels off near 29% and sustained high shear stress abundance decreases to 3% at the river mouth, this would cause polygenetic microtextures to proportionally increase in the distal samples. This is a reasonable trend due to longer transport distances propensity to increase grain fracturing resulting most commonly in polygenetic microtextures. Moreover, grain fracturing may result in the loss of sustained high shear stress microtextures through spalled fragments.

6.1.4 F/G Ratio of the Salmon River

The F/G microtexture ratio for the Salmon River displays a strong positive correlation indicative of progressive increase of fluvial and decrease of glacial microtextures with distance transported downstream (Fig. 6.2). In the Chitina River, the F/G microtexture ratio increases or decreases in response to river tributaries adding saltation length to quartz grains or glaciers intersecting the Chitina River increasing the input of glacial microtextures (Sweet and Brannan, (in press)). In the Salmon River, only one data point shows an increase when compared to the other data points. This data point corresponds to ~ 14 km downstream and occurs after the confluence of the largest of the tributaries, Texas Creek. This slight increase in fluvial influence shown by the F/G ratio at this confluence is likely due to the length and size of Texas Creek.

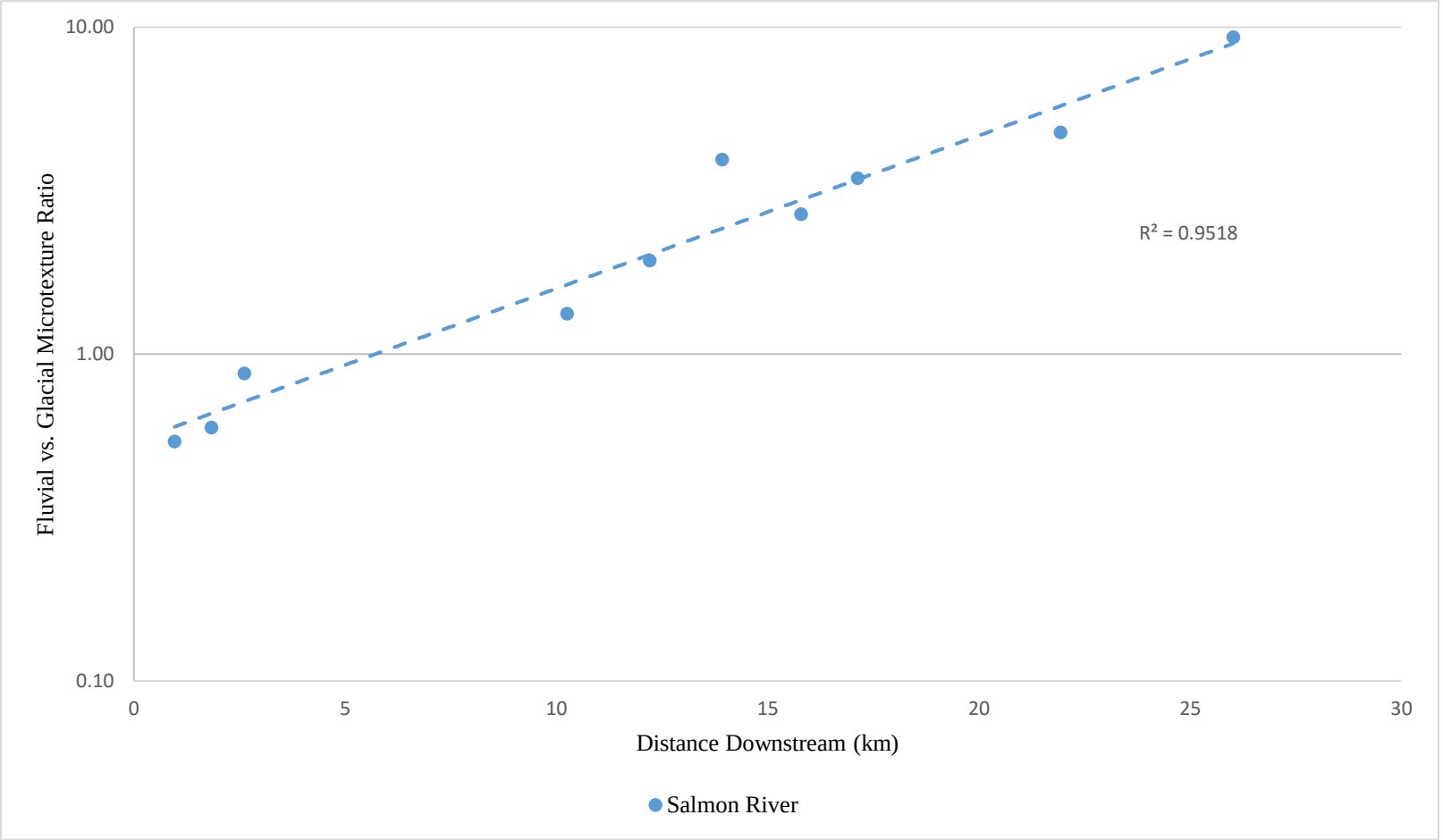

Figure 6.2: Fluvial to glacially induced microtextures ratio of the Salmon River as a function of distance downstream.

6.2 Salmon River and Chitina River Data Comparison

Salmon River microtextures display downstream trends similar to those found in the Chitina River (Brannan, 2015). The regional geology of the Chitina River is similar enough for a comparison with Salmon River samples, but hydrological characteristics of the two systems are different enough to evaluate the validity of microtextural analysis in multiple river environments. Permanent flow meters have not been established in the Chitina, but from 1955 to 1985 average flows of 1,067 m^3/s with peak discharge of 2846 m^3/s were recorded (Emery et al., 1985). Approximately half of the discharge recorded are estimated from the Chitina River and the other half from the Copper River (Emery et al., 1985). Additionally, the Chitina River watershed differs from the Salmon River in: 1) exhibiting more fluvial and glacial confluences; 2) having approximately seven times greater length (~188 km); 3) a shallower gradient (0.004 to 0.002); and 4) lacks any documented annual outburst floods (Emery, 1985; Brannan, 2015). Due to intersections of additional valley glaciers downstream in the Chitina River, the first 17 km of river transport is comparable to the Salmon River as the Salmon River does not intersect valley glaciers along its course. Comparison of the two rivers can be made to evaluate if the technique applied in these studies yields results similar enough to use in rivers with various hydrologic conditions. If the results are similar between the two systems, then the observations become much less river-specific and potentially more process-specific.

6.2.1 Sustained High Shear Stress Comparison

Proximal samples of the Chitina and Salmon River exhibit similar range of occurrence frequency for sustained high shear stress microtextures, and both systems show a negative correlation between these microtextures to distance downstream from

the glacial terminus ($R^2 = 0.53$ and $R^2 = 0.93$, respectively) (Fig. 6.3). These data suggest that the Salmon River is more efficient at overprinting the glacial signal on quartz grains. Potentially, the increased efficiency results from some of the hydrologic variations between the systems. The overall Chitina River gradient (0.004 - 0.002) is much lower than that of the Salmon River (0.10 - 0.006). The hydrologic power of the rivers is largely driven by the stream power equation which is a function of slope and discharge (Bridge and DeMicco, 2008). Additionally, degree of turbulence and grain entrainment are controlled by depth, velocity and slope (e.g. Bridge and DeMicco, 2008). The steeper slope and annual outburst flooding likely indicate that the Salmon River exerts a higher energy regime on entrained grains, and the potential to fracture is enhanced. High energy regime such as tsunamis have been recorded to increase percussion microtextures over short distances (~ 2 km) of transport (Costa et al., 2013). Fracturing of grains increases the potential removal of sustained high shear stress microtextures through spalling off fragments. If so, then the overprinting of sustained high stress microtextures should be more efficient. Other studies of proglacial systems with various characteristics are needed to test these suggestions.

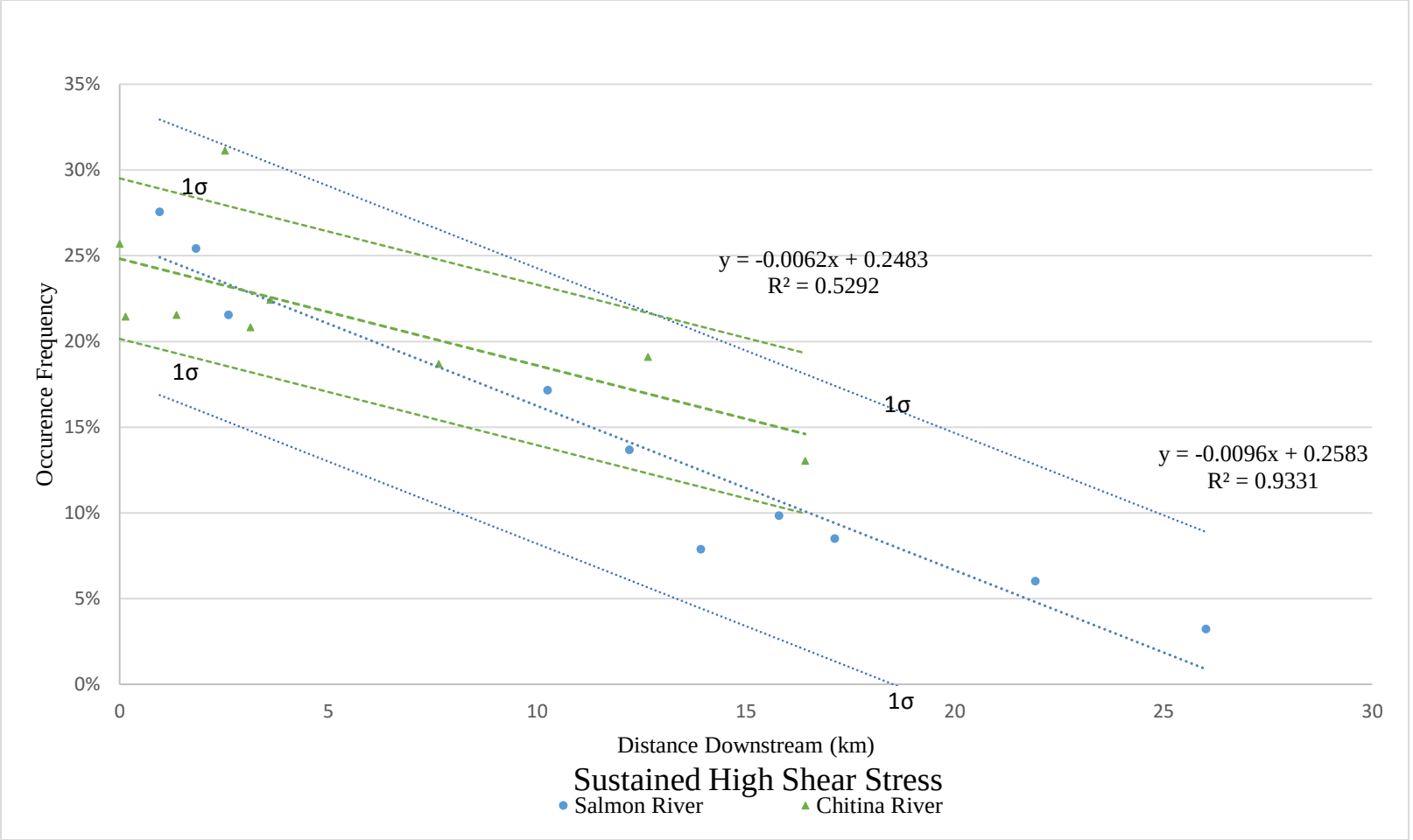

Figure 6.3: Linear regression of sustained high shear stress microtextures for the Chitina and Salmon rivers. Tripartite microtexture occurrence frequencies are shown for the rivers. The straight line equation for each data trend line and linear regression value are noted in each plot. Each graph displays one standard deviation above and below the data trend lines. Chitina River sample trend line is denoted by a dashed green line. Salmon River sample trend line is denoted by a dotted blue line.

6.2.2 Percussion Microtextures Comparison

Over the compared reaches of the Chitina and Salmon rivers the relative abundance of percussion microtextures is positively correlated to increased distance of downstream transport ($R^2 = 0.65$ and $R^2 = 0.81$, respectively). The stronger positive correlation of the Salmon River data suggests an inherent property of the river that more effectively produces percussion microtextures. As argued above for sustained high stress microtextures, the higher degree of turbulence and grain entrainment expected for the Salmon River hydraulic parameters likely resulted in more grain-to-grain interactions producing more percussion microtextures.

The above discussion of observed trends assumes that the grains in the proximal setting did not exhibit substantially different abundances in percussion microtextures. Yet, the Chitina River have initially lower values (1 to 8%) of percussion microtextures than the Salmon River (15 to 19%) (Fig. 6.4). This variance in the proximal realm suggests that some of the initial percussion transport induced features were acquired from subglacial transport. This possibility is addressed in a later section.

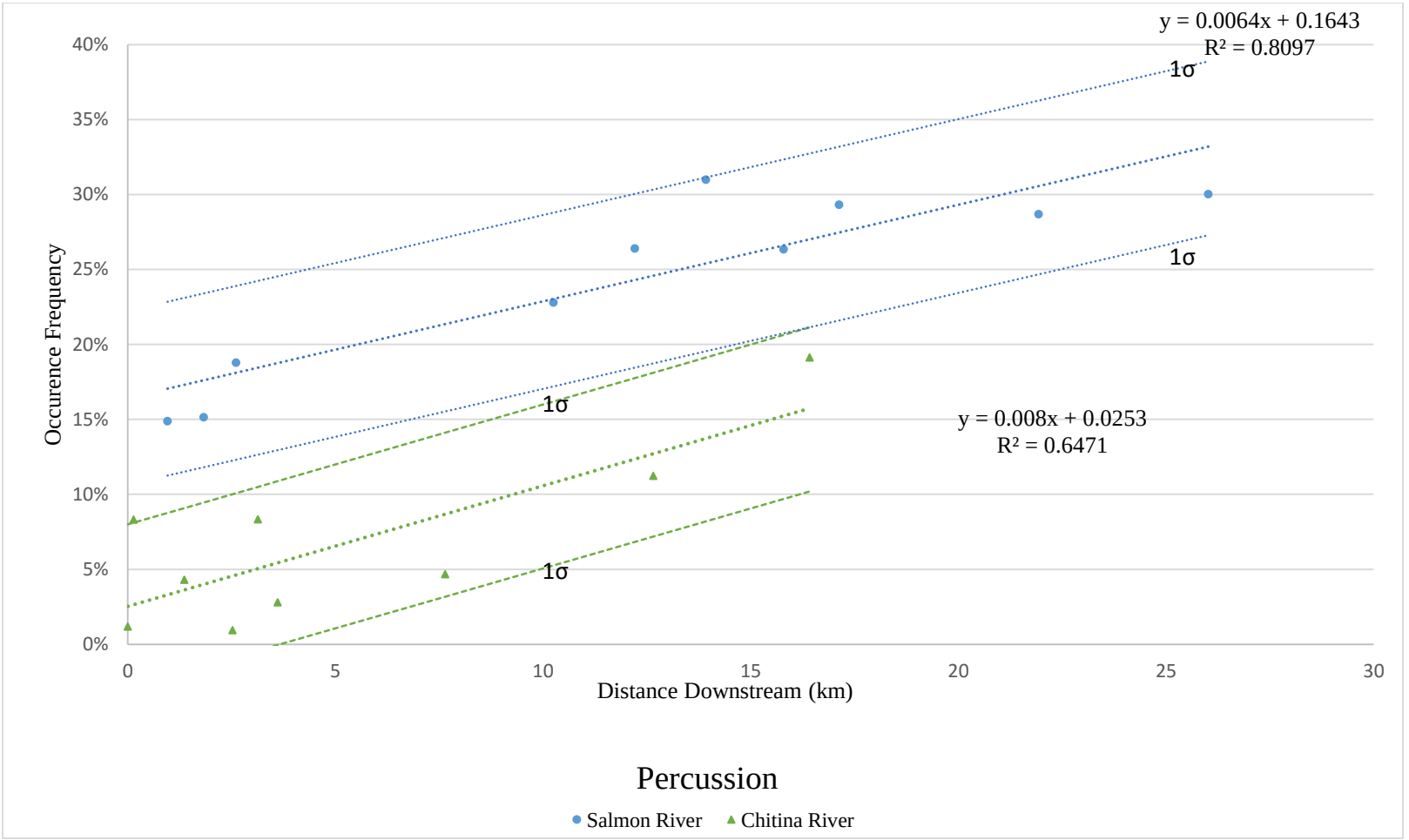

Figure 6.4: Linear regression of percussion microtextures for the Chitina and Salmon rivers. Tripartite microtextural occurrence frequency are shown for the rivers. The straight line equation for each data trend line and linear regression value are noted in each plot. Each graph displays one standard deviation above and below the data trend lines. Chitina River samples trend line is denoted by a dashed green line. Salmon River samples trend line is denoted by a dotted blue line.

6.2.3 Polygenetic Microtextures Comparison

Polygenetic microtextures show the least consistency between the Chitina River and Salmon River. In the Chitina study, no correlation ($R^2 = 0.11$) is observed whereas in the Salmon River a strong positive correlation is observed ($R^2 = 0.86$) (Fig. 6.5). The variance in polygenetic microtextures could indicate that polygenetic microtextures are truly random and do not display any relationship with distance transported, or that transport in the two rivers does not fracture grains equally. Due to the nonadherence between the two data sets, polygenetic microtextures seem to be the least useful of the tripartite suite. This result is expected given that polygenetic microtextures are not process-specific.

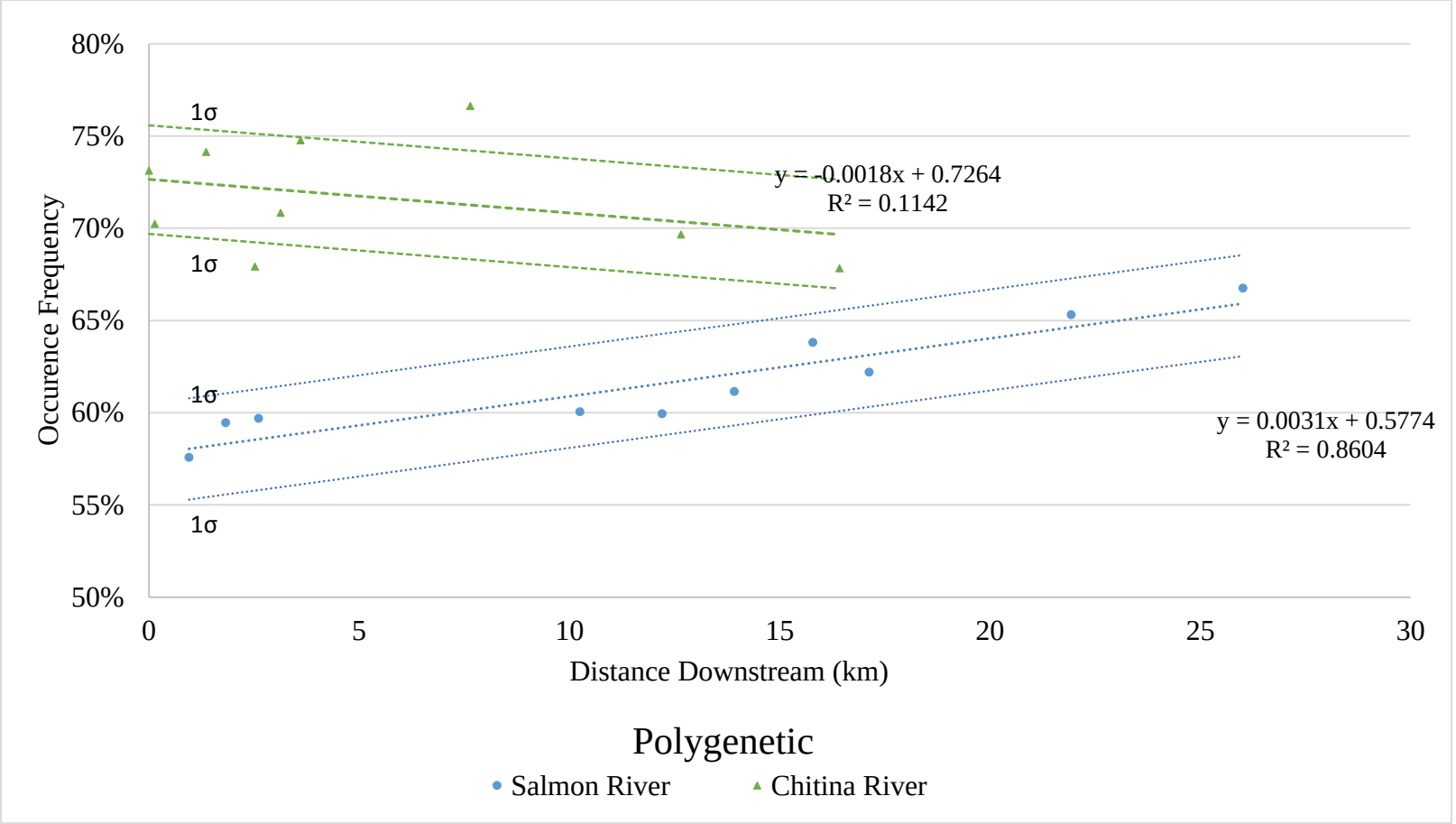

Figure 6.5: Linear regression of polygenetic microtextures for the Chitina and Salmon rivers. Tripartite microtextures occurrence frequency are shown for the rivers. The straight line equation for each data trend line and linear regression value are noted in each plot. Each graph displays one standard deviation above and below the data trend lines. Chitina River samples trend line is denoted by a dashed green line. Salmon River samples trend line is denoted by a dotted blue line.

6.2.4 Comparisons of Microtexture Occurrence Frequency for the Combined Data

Comparing the Chitina and Salmon River data sets shows that sustained high shear stress microtextures have the most consistency between the two studies (Fig. 6.3). In the regression equation for sustained high shear stress microtextures (Fig. 6.6), all data points fall within one standard deviation and exhibit a strong negative correlation (R^2 = 0.85) with distance downstream. Percussion microtextures of the combined data displays a positive correlation (R^2 = 0.62) with distance downstream (Fig. 6.6). This suggests that distance downstream has predictive capability for sustained high shear stress and percussion microtextures, assuming no other influence than distance of transport. To create a more robust analysis, additional rivers will need testing to further the accuracy or validity of this method. Nevertheless, two different river systems produce highly similar trends demonstrating the potential of the method. Polygenetic microtextures display the most random relationship when combined. No correlation (R^2 = 0.04) exists, indicating that there is no preference of polygenetic microtextures occurrence frequency with distance downstream (Fig. 6.6). The F/G ratio of the combined data from the Chitina and Salmon rivers increases linearly with distance downstream (Fig. 6.7) indicating potential predictive capability.

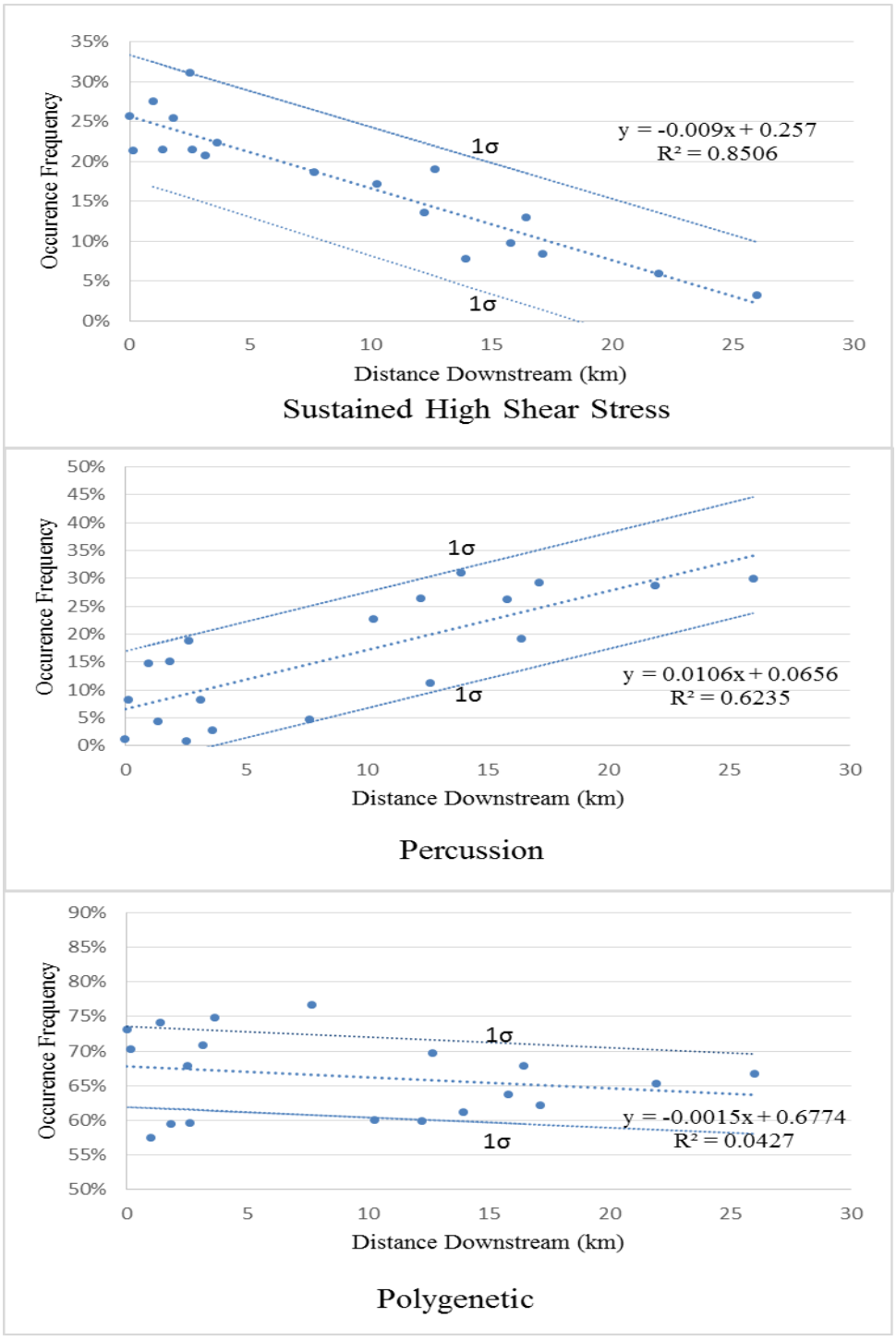

Figure 6.6: Linear regression of polygenetic, percussion, and sustained high shear stress microtextures for Chitina and Salmon rivers. Tripartite microtextures occurrence frequency are shown for the entire length of Salmon River. The straight line equation for each data trend line and linear regression value (R^2) are noted in each plot.

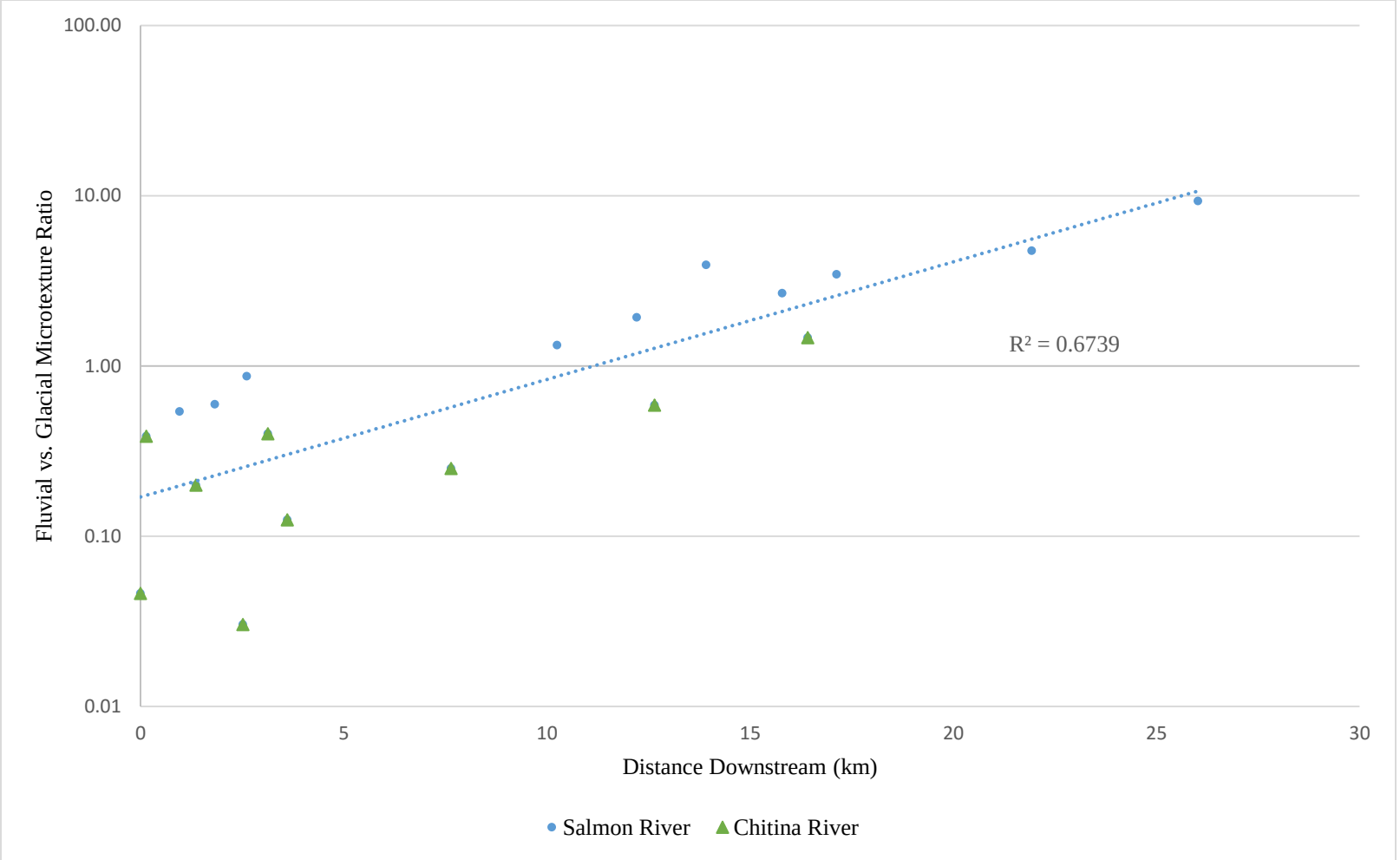

Figure 6.7: Fluvial to glacially induced microtextures ratio of the Chitina and Salmon rivers as a function of distance downstream

6.3 Assessing Subglacial River System

The Chitina River does not have documented outburst floods such as in the Salmon River. Periodically, the Salmon Glacier has a river that runs underneath from the glacial terminus to Summit Lake (~9 km). Due to this annual event, a portion of quartz grains analyzed were likely subjected to additional saltation prior to deposition at the sampling sites (SR-I through SR-III). This stretch of subglacial saltation may have resulted in the relatively elevated occurrence frequency of percussion microtextures in the Salmon River proximal samples (Fig. 6.4). If 9 km of distance is added to the cross-plots of the Salmon River data, then the y-intercept offset trends observed on figure 6.4 are reconciled (Fig. 6.8) when compared to the Chitina River data. In assessing the subglacial river system, it is assumed that Chitina River data points are taken from the "true" headwaters of the Chitina River.

6.3.1 Subglacial River Analysis of Sustained High Shear Stress Microtextures

Within the combined Chitina and Salmon River data set, a shift of 9 km for Salmon River data points would not change the fact that all data points determined are still within one standard deviation (1σ = ~8%). A strong negative correlation ($R^2 = 0.78$) of sustained high shear stress microtextures occurrence frequency to distance downstream results. All data points for the Salmon River are still within the one standard deviation bounds (Fig. 6.8) that pertain to data prior to the shift. Underlying this analysis is the assumption that all grains have experienced solely fluvial transport in the subglacial realm. Yet, it is not possible to discriminate those grains derived during the Summit Lake annual outburst versus those that are subglacial drift and thus experienced both subglacial fluvial and glacial transport. Shifting the sustained high stress microtextural data may not

be warranted. Unless other subsequent studies can provide better control, it seems unwarranted that subsequent analyses should utilize distance shifts to account for any subglacial transport in sustained high stress microtextural trends.

6.3.2 Subglacial River Analysis of Percussion Microtextures

Including additional length of fluvial transport allows for increased distance of grain saltation such that an additional 9 km of saltation transport distance added to the Salmon River data set results in little variance of the two data sets (Fig. 6.8) When Salmon River data is assessed for subglacial river length, the adherence of the two data sets show a much stronger positive correlation ($R^2 = 0.88$) of percussion microtextures occurrence frequency to distance downstream. This technique may be sensitive enough to record this specific aspect of river physiography, but more data from other glacial systems with and without subglacial fluvial transport need to be incorporated into future trend analyses to confirm this.

6.3.3 Subglacial River Analysis of Polygenetic Microtextures

Assessing the Salmon River data points after addition of subglacial river length, results in polygenetic microtextures displaying little to no correlation ($R^2 = 0.27$) to distance downstream. Additionally, five data points are outside of one standard deviation ($1\sigma = 5.7\%$). Overall, polygenetic microtextures show little difference in trends when compared to the combined Chitina and Salmon rivers data before adjusting for subglacial river length. These results are expected given the lack of process-specific transport indicators for this suite of microtextures. Shifting of the data in this way for future studies is not warranted.

Comparison of trends in polygenetic microtextures leads to the following questions for future study: 1) Do polygenetic microtextures show random correlation to distance transported?, 2) Do polygenetic microtextures increase downstream with more turbulent water flow?, 3) Do polygenetic microtextures tend to remain relatively stable throughout the fluvial system? In the Chitina data set, polygenetic microtextures exhibit poor correlation with distance downstream, but in the Salmon River these show a stronger correlation with increasing distance downstream. This may be due to the differences in hydrologic regime in the two systems, and thus will have to be fully addressed after similar work has been done on additional rivers.

6.3.4 F/G Ratio of the Salmon River to Assess Subglacial River Length

The F/G ratio was also subjected to the 9 km shift and resulted in linear regression trends with stronger correlation than in the previous non-shifted data (Fig. 6.9). As with the other shifted data, adding subglacial length tends to connect the two data sets well which suggests the technique may have merit, or alternatively that the results may be purely coincidental. To evaluate the possibility that this technique may elucidate subglacial transport, more data sets need to be incorporated.

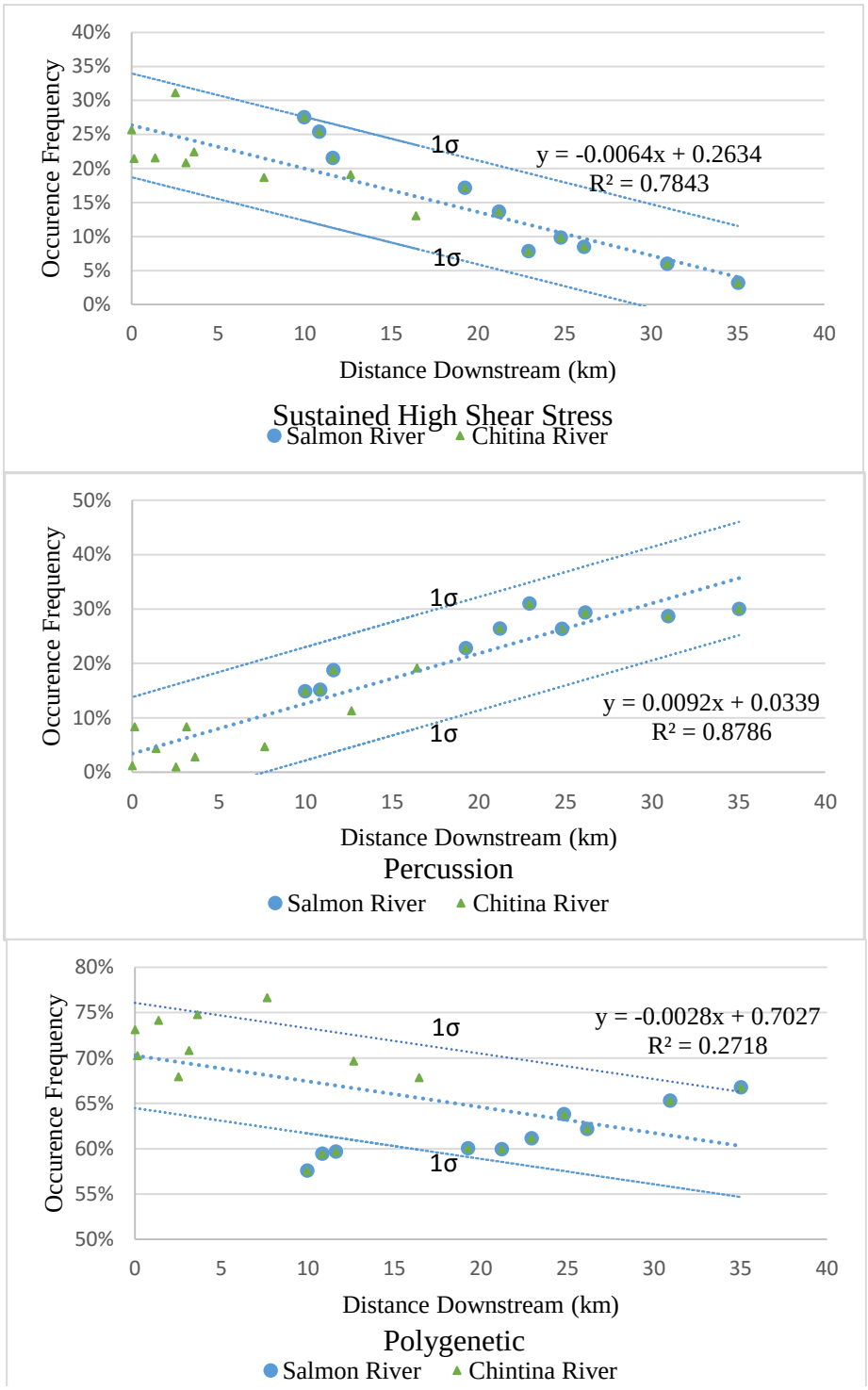

Figure 6.8: Linear regression of sustained high shear stress microtextures for the Chitina and Salmon rivers. Tripartite microtextural occurrence frequency is shown for the rivers. The straight line equation for each data trend line and linear regression value are noted in each plot. Chitina River samples trend line is denoted by a dashed green line. Salmon River samples trend line is denoted by a dotted blue line. Salmon River data points are shifted to account for 9 km of subglacial river distance.

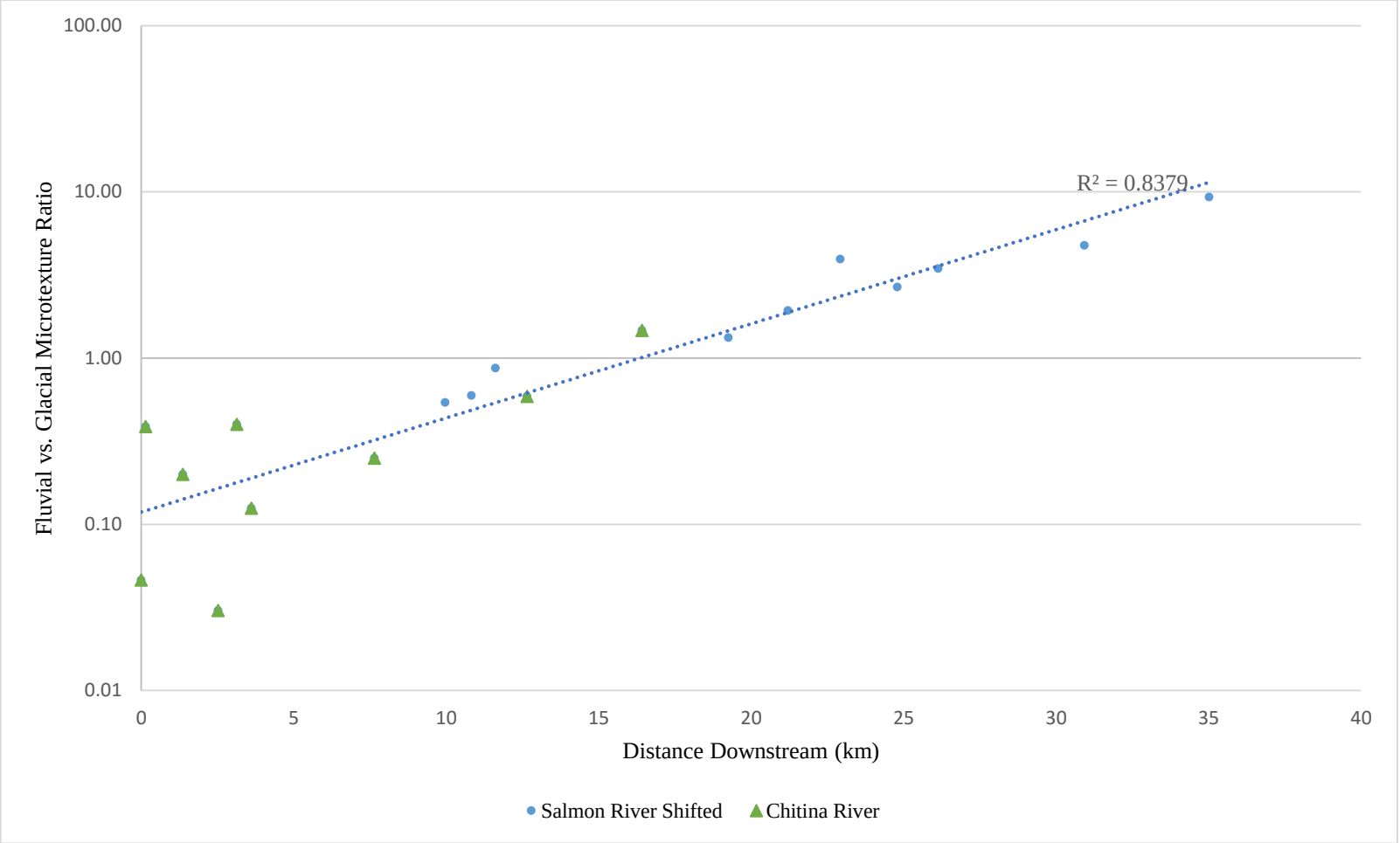

Figure 6.9: Fluvial to glacially induced microtextures ratio of the Chitina and Salmon rivers as a function of distance downstream. Salmon River data points have been shifted by 9 km in adjustment for subglacial river length

.

6.4 Application to Predict Locations of Ancient Glacial Fronts

If the relationships found within the Chitina and Salmon rivers remain consistent throughout other proglacial river systems, then applying this technique could help predict the location of ancient glacial fronts. If known glacial tills and coeval downstream river deposits plot on similar trend lines to those shown herein, then the analysis of quartz grains recovered from proglacial rivers without associated terminal moraines potentially could be used to reconstruct the glacial front. For example, if a sample analyzed under SEM imaging displays tripartite microtextures that correspond to a proglacial system at a specific downstream distance, it may be possible to locate the original glacial terminus within one standard deviation of error. Further collection of proglacial river data may decrease the range of error in this method and further refine the techniques application.

CHAPTER 7

CONCLUSIONS

Analysis of two grain-size populations found that most of the microtextures display no grain size preference. Some polygenetic microtextures such as linear steps, fracture faces, and conchoidal fractures displayed instances where a sample recorded a potentially systematic bias towards increased occurrences in the smaller grain size population (250 μm). However, when these microtextures are averaged amongst all sample localities, the variance is less than a factor or two away from unity. Overall, in this study, it appears that microtextures in both grain-size populations can be considered equally sensitive to glacial and fluvial transport processes.

Sustained high shear stress and percussion microtexture occurrence frequencies decrease or increase, respectively, with distance downstream from the Salmon Glacier terminus. Sustained high shear stress microtextures display a strong negative correlation indicating decrease of grains exhibiting glacial transport microtextures and an increase of percussion microtextures with increasing distance from the glacial front. Polygenetic microtextures also have a positive correlation, but when compared to Brannan's (2015) study on the Chitina River this correlation seems to be less significant.

Combining the data from both Chitina and Salmon rivers and evaluating the downstream trends, over the pre-glacially influenced stretch of the Chitina River (~17 km) and the full length of the Salmon River, indicates that rivers with considerably different hydraulic regimes demonstrate similar downstream trends of fluvially and

glacially induced microtextures. This relationship will require further testing to determine if this is coincidence or a commonality between multiple river systems.

Additionally, the Salmon River data provides evidence for the survivability of sustained high shear stress microtextures on quartz grains in a fluvial system up to 26 km downstream from the glacial terminus. All sustained high shear stress microtextures evaluated in this study are interpreted to undergo similar transport history and distance (i.e. Texas Glacier and Salmon Glacier deposits). In the Chitina River, sustained high shear stress microtextures survived ~188 km of river transport. However, it is unlikely the source of the sustained high shear stress microtextures was solely from the Chitina Glacier as grains were also supplied more locally through more proximal glaciers in the Chitina watershed or recycling of Pleistocene glacial drift (Sweet and Brannan, (in press)). For reasons argued herein, sustained high shear stress microtextures reported here are considered to be from the Salmon Glacier or Texas Creek Glacier. Both of these glaciers have similar transport distances and provide strong evidence that sustained high shear stress microtextures can survive 26 km of fluvial transport in a hydraulic regime similar to the Salmon River. However, by the Salmon River mouth only ~7% of grains examined for SR-X exhibited glacial microtextures indicates that complete overprinting may occur relatively quickly.

REFERENCES

Alldrick, Dani J. “Geology and Metallogeny of the Stewart Mining Camp, Northwestern British Columbia.” Vol. 85. *Province of British Columbia, Ministry of Energy, Mines and Petroleum Resources* (1993).

Alekseeva, V. A. "Micromorphology of Quartz Grain Surface as Indicator of Glacial Sedimentation Conditions: Evidence from the Protva River Basin." *Lithol Miner Resour Lithology and Mineral Resources* 40.5 (2005): 420-28.

Harold W. Baker Jr. "Environmental Sensitivity of Submicroscopic Surface Textures on Quartz Sand Grains--A Statistical Evaluation." *SEPM Journal of Sedimentary Research SEPM JSR* Vol. 46 (1976). doi:10.1306/212F707C-2B24-11D7-8648000102C1865D

Brannan, David K. “Fluvial Overprinting Of Glacially Induced Microtextures on Quartz Grains Derived From the Chitina Glacier, Alaska.” Thesis. *Texas Tech University*, (2015).

Bridge, J. S., and Robert V. Demicco. *Earth Surface Processes, Landforms and Sediment Deposits*. Cambridge, UK: Cambridge UP (2008).

Brown, Joan E. "Depositional Histories of Sand Grains from Surface Textures." *Nature* 242.5397 (1973): 396-98.

Buddington, Arthur F. “Geology of Hyder and vicinity, southeastern Alaska, with a reconnaissance of Chickamin River.” *No. 807. US Govt. Print. Off*. (1929).

Campbell, Stewart, and Ian C. Thompson. "The Palaeoenvironmental History of Late Pleistocene Deposits at Moel Tryfan, North Wales: Evidence from Scanning

Electron Microscopy (SEM)." *Proceedings of the Geologists' Association* 102.2 (1991): 123-34. doi:10.1016/s0016-7878(08)80071-5.

Clarke, Garry K.C, and Gerald Holdsworth. "Glaciers of North America—Glacier of Canada: Glaciers of the Canadian Rockies." *Satellite Image Atlas of Glaciers of the World* (2002).

Costa, P.J.M., C. Andrade, W.C. Mahaney, F. Marques Da Silva, P. Freire, M.C. Freitas, C. Janardo, M.A. Oliveira, T. Silva, and V. Lopes. "Aeolian Microtextures in Silica Spheres Induced in a Wind Tunnel Experiment: Comparison with Aeolian Quartz." *Geomorphology* 180-181 (2013): 120-29. doi: 10.106/j.geomorph.2012. 09.011

Costa, Pedro J.M., C. Andrade, A.G. Dawson, W.C. Mahaney, M.C. Freitas, R. Paris, and R. Taborda. "Microtextural Characteristics of Quartz Grains Transported and Deposited by Tsunamis and Storms." *Sedimentary Geology* 275-276 (2012): 55-69. doi: 10.1016/j.sedgeo.2012.07.013

Curry, A. M., P. R. Porter, T. D. L. Irvine-Fynn, G. Rees, T. B. Sands, and J. Puttick. "Quantitative Particle Size, Microtextural and Outline Shape Analyses of Glacigenic Sediment Reworked by Paraglacial Debris Flows." *Earth Surf. Process. Landforms Earth Surface Processes and Landforms* 34.1 (2009): 48-62. doi:10.1002/esp.1688.

Davaris, Aimee, “Southeast Alaska Jokulhlaups Report, National Weather Service Juneau Forecast Center. Alaska DOT/PF, Alaska State Transportation Improvements

Plan" *State of Alaska, Department of Transportation and Public Facilities*. (2006-2009).

D'orsay, A. M., and H. W. Van De Poll. "Comment and Reply on "Quartz-grain Surface Textures: Evidence for Middle Carboniferous Glacial Sediment Input to the Parrsboro Formation of Nova Scotia"." *Geol Geology* 14.1 (1986): 93. doi: 10.1130/0091-7613(1985)

Emery, Phillip A., Stanley H. Jones, and Roy L. Glass. "Water Resources of the Copper River Basin, Alaska." *U.S. Geological Survey Hydrologic Investigations Atlas 686* (1985).

Grove, Edward W. "Geology and Mineral Deposits of the Stewart Area." *Bulletin,* (1971):58.

Grove, Edward W. "Geology and Mineral Deposits of the Unuk River-Salmon River-Anyox Area." *Bulletin, ISSN* 226.7497 (1986): 63.

Helland, P. E., and R. F. Diffendal. "Probable Glacial Climatic Conditions in Source Areas during Deposition of Parts of the Ash Hollow Formation, Ogallala Group (late Tertiary), of Western Nebraska." *American Journal of Science* 293.8 (1993): 744-57. doi:10.2475/ajs.293.8.744.

Immonen, Ninna, Kari Strand, Antti Huusko, and Juha Pekka Lunkka. "Imprint of Late Pleistocene Continental Processes Visible in Ice-rafted Grains from the Central Arctic Ocean." *Quaternary Science Reviews* 92 (2014): 133-39. doi:10.1016/j. quascirev.2014.01.008.

Jackson, Gary. "Stratigraphy and Paleohydraulic Analysis of Glacial and Meltwater Sediments in the Mesa Del Caballo Area, Sierra De Santo Domingo, Venezuelan

Andes." *In: Mahaney, W.C., and Kalm, V. (eds.), Field Guide for the International Conference on Quaternary Glaciation and Paleoclimate in the Andes Mountains, Quaternary Surveys, Toronto, Ontario,* (1996).

Johnson, W. Hilton, and Ardith K. Hansel. "Wisconsin Episode Glacial Landscape of Central Illinois: A Product of Subglacial Deformation Processes?" *Special Paper 337: Glacial Processes Past and Present* (1999): 121-35. doi:10.1130/0-8137-2337-x.121.

Keiser, Leslie J., Gerilyn S. Soreghan, and Michal Kowalewski. "Use of Quartz Microtextural Analysis to Assess Possible Proglacial Deposition For the Pennsylvanian–Permian Cutler Formation (Colorado, U.S.A.)." *Journal of Sedimentary Research* 85.11 (2015): 1310-322.

Khalaf, S. Al-Saleh F. I. "Surface Textures of Quartz Grains from Various Recent Sedimentary Environments in Kuwait." *SEPM Journal of Sedimentary Research SEPM JSR* Vol. 52 (1982). Doi: 10.1306/212f7f18-2b24-11d7-8648000102c1865d.

Kirshner, Alexandra E., and John B. Anderson. "Cenozoic Glacial History of the Northern Antarctic Peninsula: A Micromorphological Investigation of Quartz Sand Grains." *Tectonic, Climatic, and Cryospheric Evolution of the Antarctic Peninsula Special Publications Anderson/Tectonic, Climatic, and Cryospheric Evolution of the Antarctic Peninsula* (2013): 153-65.

Krinsley, David H., and John Charles Doornkamp. *Atlas of Quartz Sand Surface Textures*. Cambridge: Cambridge UP, 1973.

Krinsley, D., and T. Takahashi. "Surface Textures of Sand Grains: An Application of Electron Microscopy." *Science* 135.3507 (1962): 923-25.

Krinsley, David H., and Jack Donahue. "Environmental Interpretation of Sand Grain Surface Textures by Electron Microscopy." *Geol Soc America Bull Geological Society of America Bulletin* 79.6 (1968): 743. Doi: 10.1130/0016- 7606(1968)79 [743:eiosgs]2.0.co;2.

Lindé, Krister, Elżbieta Mycielska-Dowgiałło, Krister Linde, and Elzbieta Mycielska-Dowgiallo. "Some Experimentally Produced Microtextures on Grain Surfaces of Quartz Sand." *Geografiska Annaler. Series A, Physical Geography* 62.3/4 (1980): 171. doi: 10.2307/520676

Mahaney, William C., Graeme Claridge, and Iain Campbell. "Microtextures on Quartz Grains in Tills from Antarctica." *Palaeogeography, Palaeoclimatology, Palaeoecology* 121.1-2 (1996): 89-103. doi:10.1016/0031-0182(95)00069-0

Mahaney, William. C., W. Vortisch, and P. J. Julig. "Relative Differences between Glacially Crushed Quartz Transported by Mountain and Continental Ice; Some Examples from North America and East Africa." *American Journal of Science* 288.8 (1988): 810-26. doi: 10.2475/ajs.288.8.810

Mahaney, William C., and James M. Dohm. "The 2011 Japanese 9.0 Magnitude Earthquake: Test of a Kinetic Energy Wave Model Using Coastal Configuration and Offshore Gradient of Earth and beyond." *Sedimentary Geology* 239.1-2 (2011): 80-86. doi:10.1016/j.sedgeo.2011.06.001.

Mahaney, William C., and Volli Kalm. "Comparative Scanning Electron Microscopy

Study of Oriented till Blocks, Glacial Grains and Devonian Sands in Estonia and Latvia." *Boreas* 29, no. 1 (2000): 35-51. doi:10.1111/j.1502-3885.2000.tb01199.x.

Mahaney, William C., and Volli Kalm. "Scanning Electron Microscopy of Pleistocene Tills in Estonia." *Boreas* 24, no. 1 (1995): 13-29. doi:10.1111/j.1502-3885.1995.tb00624.x.

Mahaney, William. C., and Volli Kalm, eds. "*Field Guide for the International Conference on Quaternary Glaciation and Paleoclimate in the Andes Mountains (and Surrounding Tropical, Subtroopical and Middle Latitude Mountains), June 21-July 1, 1996*." Quaternary Surveys, (1996).

Mahaney, William C., and William Andres. "Scanning Electron Microscopy of Quartz Sand from the North-Central Saharan Desert of Algeria." *Zeitschrift Fur Geomorphologies* (1996): 179-92.

Mahaney, William C., and Wolfgang Andres. "Glacially Crushed Quartz Grains in Loess as Indicators of Long-distance Transport from Major European Ice Centers during the Pleistocene." *Boreas* 20, no. 3 (1991): 231-39. doi:10.1111/j.1502-3885.1991.tb00153.x.

Mahaney, William C., Andrew Stewart, and Volli Kalm. "Quantification of SEM Microtextures Useful in Sedimentary Environmental Discrimination." *Boreas* 30, no. 2 (2001): 165-71. doi:10.1111/j.1502-3885.2001.tb01220.x.

Mahaney, William C. "*Atlas of Sand Grain Surface Textures and Applications*." Oxford, U.K., Oxford University Press (2002).

Mahaney, William C. "Pleistocene and Holocene Glacier Thicknesses, Transport

Histories and Dynamics Inferred from SEM Microtextures on Quartz Particles." *Boreas* 24, no. 4 (1995): 293-304. doi:10.1111/j.1502-3885.1995.tb00781.x.

Manley, W.F., and Kaufman, D.S. “Alaska PaleoGlacier Atlas: Institute of Arctic and Alpine Research (INSTAAR).” *University of Colorado*, http://instaar.colorado.edu/QGISL/ak_paleoglacier_atlas, v. 1. (2002)

Mathews, W. H. "Two Self-dumping Ice-dammed Lakes in British Columbia."*Geographical Review* (1965): 46-52. doi: 10.2307/212854

Margolis, Stanley V. "Electron Microscopy of Chemical Solution and Mechanical Abrasion Features on Quartz Sand Grains." *Sedimentary Geology*2.4 (1968): 243-256. doi:10.1016/0037-0037(68)90002-X

Mazzullo, Jim, and Christine Ritter. "Influence of Sediment Source on the Shapes and Surface Textures of Glacial Quartz Sand Grains." *Geology Geol* 19, no. 4 (1991): 384. doi:10.1130/0091-7613(1991)0192.3.co;2.

Mazzullo, Jim. "Origin Shapes in the St. Peter Sandstone: Determination by Fourier Shape Analysis and Scanning Electron Microscopy." *In Marshall, J.R. (ed.) Clastic Particles. Van Nostrand Reinhold, New York*: 302-13 (1983).

Osborn, G., and B. Luckman. "Holocene Glacier Fluctuations in the Canadian Cordillera (Alberta and British Columbia)." *Quaternary Science Reviews* 7.2 (1988): 115-28.

Post, Austin, and Lawrence R. Mayo. “Glacier Dammed Lakes and Outburst Floods in Alaska.” *Washington: US Geological Survey* (1971).

Strand, Kari, Sandra Passchier, and Jari Näsi. "Implications of Quartz Grain Microtextures for Onset Eocene/Oligocene Glaciation in Prydz Bay, ODP Site

1166, Antarctica." *Palaeogeography, Palaeoclimatology, Palaeoecology*198.1 (2003): 101-111. doi: 10.1016/S0031-0182(03)00396-1

Strand, Kari, and Ninna Immonen. "Dynamics of the Barents-Kara Ice Sheet asRrevealed by Quartz Sand Grain Microtextures of the Late Pleistocene Arctic Ocean Sediments." *Quaternary Science Reviews* 29.25 (2010): 3583-3589.

Sweet, D.E. and Brannan, D.K., "Proportion of Glacially to Fluvially Induced Quartz Grain Microtextures Along the Chitina River, SE Alaska." *Journal of Sedimentary Research.* (in press).

Sweet, D. E., and G. S. Soreghan. "Application of Quartz Sand Microtextural Analysis to Infer Cold-Climate Weathering for the Equatorial Fountain Formation (Pennsylvanian-Permian, Colorado, U.S.A.)." *Journal of Sedimentary Research* 80, no. 7 (2010): 666-77. doi:10.2110/jsr.2010.061.

Sweet, D. E., and G.S. Soreghan. "Polygonal Cracking in Coarse Clastics Records Cold Temperatures in the Equatorial Fountain Formation (Pennsylvanian–Permian, Colorado)." *Palaeogeography, Palaeoclimatology, Palaeoecology* 268, no. 3-4 (2008): 193-204. doi:10.1016/j.palaeo.2008.03.046.

USACE. "Alaska Community Erosion Survey." OMB approved number 07100001, expires September 30, 2009 completed by Carol Denton, Hyder city administrator, on (February 21, 2008).

Van Hoesen, John G., and Richard L. Orndorff. "A Comparative SEM Sstudy on the Micromorphology of Glacial and Nonglacial Clasts with Varying Age and Lithology." *Canadian Journal of Earth Sciences* 41.9 (2004): 1123-1139.

Vos, Koen, Noël Vandenberghe, and Jan Elsen. "Surface Textural Analysis of Quartz Grains by Scanning Electron Microscopy (SEM): From Sample Preparation to Environmental Interpretation." *Earth-Science Reviews* 128 (2014): 93-104. doi:10.1016/j.earscirev.2013.10.013

Whalley, William B., and Chester C. Langway Jr. "A Scanning Electron Microscope Examination of Subglacial Quartz Grains from Camp Century core, Greenland--a Preliminary Study." *Journal of Glaciology* 25 (1980): 125-131.

Witus, Alexandra E., Carolyn M. Branecky, John B. Anderson, Witold Szczuciński, Dustin M. Schroeder, Donald D. Blankenship, and Martin Jakobsson. "Meltwater Intensive Glacial Retreat in Polar Environments and Investigation of Associated Sediments: Example from Pine Island Bay, West Antarctica." *Quaternary Science Reviews* 85 (2014): 99-118. doi:10.1016/j.quascirev.2013.11.021.